COMBINATION OF CONVENTIONAL REGULARIZATION METHODS AND GENETIC ALGORITHMS FOR SOLVING THE INVERSE PROBLEM OF ELECTROCARDIOGRAPHY

A THESIS SUBMITTED TO
THE GRADUATE SCHOOL OF APPLIED MATHEMATICS
OF
MIDDLE EAST TECHNICAL UNIVERSITY

BY

SEDAT SARIKAYA

IN PARTIAL FULFILLMENT OF THE REQUIREMENTS
FOR
THE DEGREE OF MASTER OF SCIENCE
IN
SCIENTIFIC COMPUTING

FEBRUARY 2010

Approval of the thesis:

COMBINATION OF CONVENTIONAL REGULARIZATION METHODS AND GENETIC ALGORITHMS FOR SOLVING THE INVERSE PROBLEM OF ELECTROCARDIOGRAPHY

submitted by **SEDAT SARIKAYA** in partial fulfillment of the requirements for the degree of **Master of Science in Department of Scientific Computing**, **Middle East Technical University** by,

Prof. Dr. Ersan Akyıldız _____
Director, Graduate School of **Applied Mathematics**

Prof. Dr. Bülent Karasözen _____
Head of Department, **Scientific Computing**

Assist. Prof. Dr. Yeşim Serinağaoğlu Doğrusöz _____
Supervisor, **Department of Electrical and Electronics Engineering, METU**

Prof. Dr. Gerhard-Wilhelm Weber _____
Co-Supervisor, **Department of Scientific Computing, METU**

Examining Committee Members:

Assoc. Prof. Dr. İnci Batmaz _____
Department of Statistics, METU

Assist. Prof. Dr. Yeşim Serinağaoğlu Doğrusöz _____
Department of Electrical and Electronics Engineering, METU

Prof. Dr. Gerhard-Wilhelm Weber _____
Department of Scientific Computing, METU

Assist. Prof. Dr. İlkay Ulusoy _____
Department of Electrical and Electronics Engineering, METU

Assist. Prof. Dr. Hakan Öktem _____
Department of Scientific Computing., METU

Date: _____

I hereby declare that all information in this document has been obtained and presented in accordance with academic rules and ethical conduct. I also declare that, as required by these rules and conduct, I have fully cited and referenced all material and results that are not original to this work.

Name, Last name: SEDAT SARIKAYA

Signature :

ABSTRACT

COMBINATION OF
CONVENTIONAL REGULARIZATION METHODS AND GENETIC ALGORITHMS FOR SOLVING THE INVERSE PROBLEM OF ELECTROCARDIOGRAPHY

Sarıkaya, Sedat

M.Sc., Department of Scientific Computing

Supervisor : Assist. Prof. Dr. Yeşim Serinağaoğlu Doğrusöz

Co-Supervisor: Prof. Dr. Gerhard-Wilhelm Weber

February 2010, 73 pages

Distribution of electrical potentials over the surface of the heart, i.e., the epicardial potentials, is a valuable tool to understand whether there is a defect in the heart. However, it is not easy to detect these potentials non-invasively. Instead, body surface potentials, which occur as a result of the electrical activity of the heart, are measured to diagnose heart defects. However the source electrical signals loose some critical details because of the attenuation and smoothing they encounter due to body tissues such as lungs, fat, etc. Direct measurement of these epicardial potentials requires invasive procedures. Alternatively, one can reconstruct the epicardial potentials non-invasively from the body surface potentials; this method is called the inverse problem of electrocardiography (ECG). The goal of this study is to solve the inverse problem of ECG using several well-known regularization methods and using their combinations with genetic algorihm (GA) and finally compare the performances of these methods. The results show that GA can be combined with the conventional regularization methods and their combination improves the regularization of ill-posed inverse ECG problem.

In several studies, the results show that their combination provide a good scheme for solving the ECG inverse problem and the performance of regularization methods can be improved further. We also suggest that GA can be initiated succesfully with a training set of epicardial potentials, and with the optimum, over- and under-regularized Tikhonov regularization solutions.

Keywords: Electrocardiography, Inverse Problems, Inverse Problem of Electrocardiography, Regularization Methods, Genetic Algorithm

ÖZ

TERS ELEKTROKARDİYOGRAFİK PROBLEMLERİN ÇÖZÜMÜ İÇİN
GELENEKSEL DÜZENLİLEŞTİRME YÖNTEMLERİ VE
GENETİK ALGORİTMALARIN BİRLEŞTİRİLMESİ

Sarıkaya, Sedat
Yüksek Lisans, Bilimsel Hesaplama Bölümü
Tez Yöneticisi : Assist. Prof. Dr. Yeşim Serinağaoğlu Doğrusöz
Ortak Tez Yöneticisi: Prof. Dr. Gerhard-Wilhelm Weber

Şubat 2010, 73 sayfa

Kalp üzerindeki elektriksel potansiyellerinin (epikard potansiyelleri) dağılımı, kalpte bir sorun olup olmadığını anlamakta kullanılan değerli bir araçtır. Fakat bu potansiyelleri invaziv girişim yapmadan ölçmek kolay değildir. Bunun yerine kalpteki elektriksel aktivitelere bağlı olarak oluşan vücut yüzeyi potansiyelleri ölçülerek, kalp hastalıkları tespit etmekte kullanılır. Fakat kalpteki elektriksel sinyaller vücut yüzeyine ulaşana kadar, kalp etrafındaki dokular ya da organların, örneğin akciğer, yağ vs., sinyalleri yumuşatması yada zayıflatmasından dolayı bazı önemli detaylarını kaybederler. Kalp potansiyellerini doğrudan ölçmek için ise invaziv bir yöntem kullanılması gerekir. Alternatif olarak, vücut yüzeyinden ölçülen potansiyellerden kalp potansiyelleri invaziv olmayan bir şekilde kestirilebilirler, bu yöntem ters elektrokardiografi (EKG) olarak adlandırılır. Bu tezde, ters EKG probleminin bazı iyi bilinen düzenlileştirme yöntemleriyle ve bu yöntemlerin genetik algoritma ile birleştirilmesiyle çözülmesi, sonra da kullanılan çözüm yöntemlerinin başarımlarının karşılaştırılması amaçlanmıştır. Alınan sonuçlar genetik algoritmanın düzenlileştirme yöntemleri ile beraber ters problem çözümlerinde kullanılabileceğini ve uygulanan birleştirme yönteminin düzenlileştirmeyi iyileştirdiğini göstermiştir. Yapılan bazı çalışmalarda iki yöntemin birleştirilmesi ile genetik algoritmaların kötü konumlanmış EKG problemlerinin çözümünde düzenlileştirme yöntemlerine önemli katkısı

olacağı önerilmektedir. Biz bu çalışmalara ek olarak kalp potansiyel eğitim kümelerinin ve Tikhonov düzenlileştirmesi yönteminde optimum, fazla ve az düzenlileştirme kullanarak elde edilen çözümlerin GA için başlangıç popülasyonu olarak kullanılabileceğini ve böylece daha doğru çözümlerin elde edilebileceğini önermekteyiz.

Anahtar Kelimeler: Elektrokardiografi, Ters Problemler, Elektrokardiografi Ters Problemi, Düzenlileştirme Metodları, Genetik Algoritma

To my family

ACKNOWLEDGMENTS

I would like to thank all those people who have helped in the preparation of this study. I am grateful to Assist. Prof. Dr. Yeşim Serinağaoğlu Doğrusöz for her motivation and support that provided me determination and power throughout this study.

Special thanks to my co-advisor Prof. Dr. Gerhard-Wilhelm Weber for his support and kindness.

I would also like to thank Assoc. Prof. Dr. İnci Batmaz, Assist. Prof. Dr. İlkay Ulusoy and Assist. Prof. Dr. Hakan Öktem for their valuable support and time they spared for me.

And, I would like to thank my family for their endless support, hope, care and help. I would like to thank my wife Yıldız Güneş Sarıkaya and my little daugther Sezen Sarıkaya for their patience and love and to my mother Güler Sarıkaya and my father Celal Sarıkaya for their efforts. I would like to dedicate this study to my all family whom I am proud of.

Thank you...

TABLE OF CONTENTS

LIST OF TABLES

TABLES

LIST OF FIGURES

FIGURES

CHAPTER 1

INTRODUCTION

1.1 Motivation

Heart diseases are the main cause of death all over the world in modern society. For example, heart diseases accounted for approximately 30% of all deaths around the world in the year 2007 [1]. Therefore it is very important to diagnose the heart related illnesses successfully. Such illnesses can be diagnosed from epicardial potential distributions. The electrocardiogram was recorded firstly by A. Waller [2] in 1887. After the appearance of the electrocardiogram, the researchers have been trying to understand the electrical activity of the heart by studying recorded potentials on the body surface by placing electrodes on the torso surface. It is very important to improve the understanding of the functioning of the heart, which allows a clinician to identify the defects occuring in the heart and therapy for it. Also, it reduces the time and costs to diagnose the defects. By locating electrodes on the body surface, the occurent potential difference between the electrodes gives an indication of the existance of electrical activities in the heart and these electrical activities can be displayed as an electrocardiogram using special instruments. The electrical potentials mesured from body surface vary continuously throughout each cardiac cycle. However, the tissue between the heart and the body surface attenuates and smooths the electrical potentials of the heart, and some important details may be lost in the body surface potential measurements. The aim of the inverse problem of Electrocardiography (ECG) is to reconstruct the electrical activity of the heart from body surface potentials in a non-invasive way, and hence capture the details lost in the body surface measurements. Inverse problems generally consider the reconstruction of the cause, i.e., the set of parameters, using the effects, i.e., the measurements as opposed to forward problems that deal with the prediction of these effects for a known cause.

In this study we focused on the inverse problem of ECG with the epicardial potential distributions as the cardiac source models. Solving this kind of problem is difficult because of its ill-posed nature. One can reduce the effects of this ill-posedness by applying regularization on the solution; i.e., by imposing constraints on the solution.

The main aim of this study is to solve the inverse ECG problem by using some of the well-known regularization methods, and to combine these regularized solutions with genetic algorithm (GA). The results of conventional regularization methods (without GA) are compared among themselves and with the results that are obtained by combining these methods with the GA to see the contributions of GA to the regularization of the ill-posed inverse ECG problem.

In literature, several regularization methods were proposed for solving inverse ECG problems such as Tikhonov Regularization, Truncated Singular Value Decomposition (TSVD), Truncated Generalized Singular Value Decomposition (TGSVD), Least Squares QR (LSQR), Bayesian Maximum a Posteriori (MAP) method, etc. Recently, several studies have been done to solve the inverse ECG problem by combining regularization methods and GA. In these studies, the results of the regularization methods were used as the initial population (IP) for the GA. In order to run the fitness function of the GA, they compared the iteration results with the known (exact) epicardial potentials. In this study, we solved the inverse problem of ECG with several regularization methods which were proposed in literature and we extended the combination of regularization methods with the GA. The contributions of thesis can be listed as follows:

- We used the combination of the GA with two other regularization methods (TSVD and Bayesian MAP Estimation) different from literature studies,
- We used training set of epicardial potentials as the IP for the GA,
- We employed the GA to the results of regularization methods which chose regularization parameters in a range of optimum, under- and over-regularized value region,
- We implemented a graphical user interface to run different regularization methods and also run the GA for different parameters (see Appendix A, C).

1.2 Scope of the Thesis

This thesis is composed of seven main chapters and an Appendix. Brief contents are given below:

Chapter 1 Introduction of the thesis. The objectives and outlines of the study is given in this chapter.

Chapter 2 The background information about ECG and the heart. The previous works on the ECG literature.

Chapter 3 Theory, methods and approaches used in the study.

Chapter 4 Contributions of GA to regularize ill-posed inverse ECG problem and combination of GA with conventional regularization methods.

Chapter 5 Simulation results for comparison of the regularization methods and GA results. The results are discussed at the end of this chapter.

Chapter 6 A brief summary, and conclusions.

CHAPTER 2

MEDICAL BACKGROUND

There are many studies in literature about the heart diseases and how to get information about them without invasive operations to the heart. Also there are lots of information about the heart, its functioning, and its contributions to the body cardiovascular system. In this chapter we describe the heart anatomy and the elecrical activities occuring in the heart.

2.1 The Heart Anatomy

The human heart, center of cardiovascular system, is located in the chest between the lungs (Figure 2.1). Its weight is typically between 250 and 300 g [3].

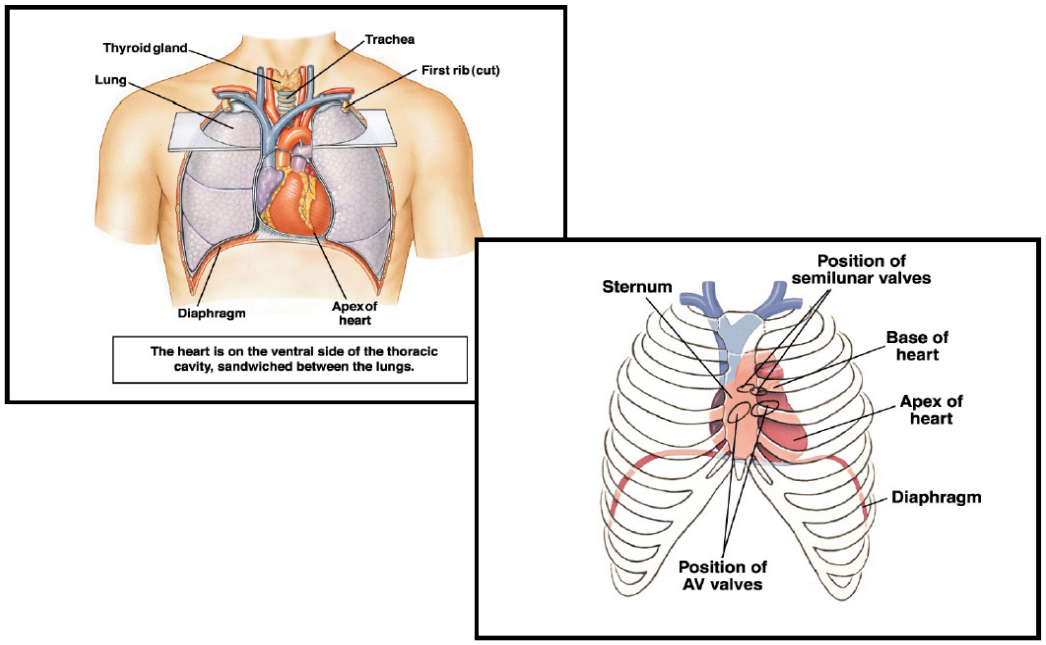

Figure 2.1 The position of heart in human torso [3]

The walls of the heart consist of cardiac muscle tissue which is called the myocardium. The function of the heart is to pump the blood through the body, thus enabling the transportation of

nutrient materials as well as oxygen to the other organs of the body. The blood circulation system consists of two main parts.

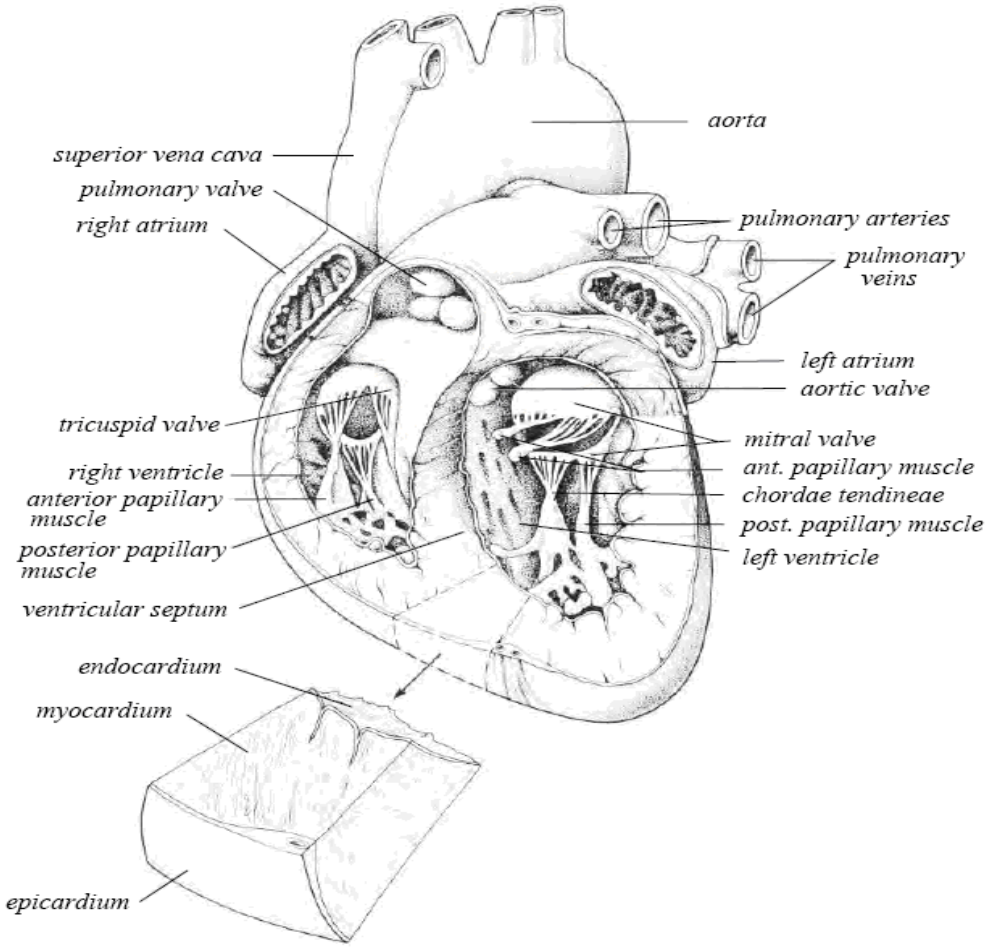

Figure 2.2 The Heart Anatomy [3]

The pulmonary circulation carries the blood, which is poor with oxygen, to the lungs to become rich it with oxygen. The systemic circulation is responsible for the transportation of blood saturated with oxygen throughout the body. In Figure 2.2, the heart anatomy is shown, which is a part of the circulation system [4]. There are four chambers in the heart whose walls are thick and muscular. Left and right ventricles are the two chambers of the heart which are located in the bottom part of the heart and their functions are to pump blood out of the heart. The remaning chambers located in the upper part of the heart are called the right and left atria. The functions of the atrias are to receive the blood into the heart. The left ventricle has a smaller volume than the right one [3].

The oxygen-poor blood is pumped by the right ventricle through the valve into the left and right arteries. These arteries carry the blood to the lungs to become it rich with oxygen. Then the blood is passing through the left atrium and reaches the left ventricle. The left ventricle has a relatively thick wall which produces a high pressure to pump the arterial blood which is rich with oxygen throughout the body. The atria are separated from the ventricles with the mitral and tricuspid valves, which prevent the flowing of the blood inversely. The pupillary muscles support these valves. The myocardium (ventricular) is supplied with blood by the coronary vessels. There is an oxygen deficiency if there is a defect in the myocardial tissue. It causes a blockage of the blood inflow and myocardial disease (infarction) [5].

2.2 Electrophysiology of the Heart

A small pulse of electric current initiates a heart beat. This impulse (electricity) spreads in the different tissues of the heart quickly and causes a contraction in the heart muscle. The heart muscle produces and transfers the electrical excitation as well as those reacting on the excitation with contraction [6]. The electrical activaties in the heart are normally generated in the sinoatrial node (SA-node), afterwards the signals pass through both atria to the atrio-ventricular node (AV-node).

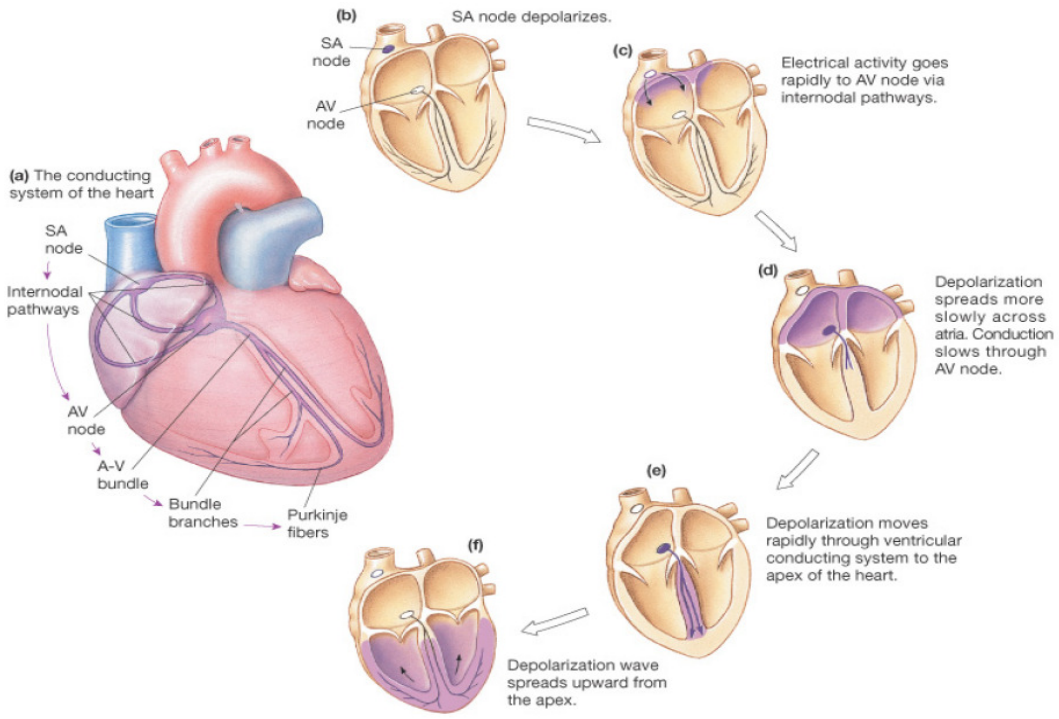

Figure 2.3 Electrical impulse flowing in the heart [6]

The AV-node behaves an alternative to SA-node if it does not work properly or there is a blockage to its impulses. Then, the excitation is carried to the ventricular myocardium by the cardiovascular conduction system. The flow of electrical impulses throughout the heart is illustrated in Figure 2.3. The appearing of the excitation in the heart can be carried throughout the myocardium causing the contraction of the heart. The electrophysiology of myocardial cells is explained by their transmembrane voltage (TMV) [47], which means that the potential difference between the intra- and extra-cellular heart spaces and it can be defined as follows:

$$V_m = \Phi_i - \Phi_e \tag{2.1}$$

where V_m is the TMV and Φ_i and Φ_e are symbolized for the intra- and extra-celluar potentials, respectively. The TMV changes between the -80 mV (rest) and +20 mV (activation) (see more details in Appendix B for all information in this section).

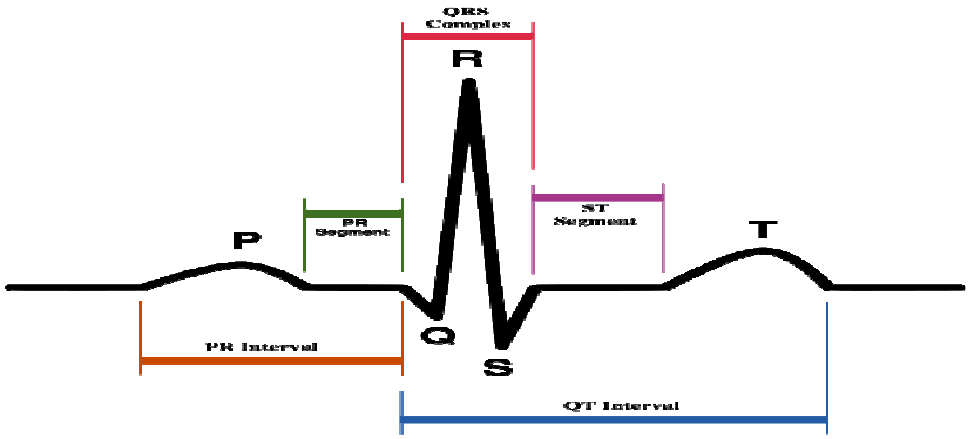

Figure 2.4 The ECG waveform [6]

The activation propagation throughout the ventricles corresponds to the QRS-complex[1] (Figure 2.4) of ECG. After the depolarization follows the plateau phase, which means that the TMV stays more or less constant. During this phase the mechanical contraction of the heart takes place. Afterwards the repolarization phase comes, during which the TMV changes back to -80 mV. This phase is reproduced by the T-wave of ECG (Figure 2.4). After the electrical relaxation follows also the mechanical relaxation of the heart. In Figure 2.5, the membrane potential changes are shown phase by phase. The change in TMV after the activation of excitable cell is called action potential. Different tissues of the heart have different action potential curves. There

[1] The **QRS complex** is a recording of a single heartbeat on the ECG that corresponds to the depolarization of the right and left ventricles.

is a potential distribution measured from the body surface due to the action potentials. The summation of these potentials can be measured by electrodes from body surface, which can be shown in a graphical result called electrocardiography. In this graphical result, there are different waves (P,Q,R,S,T) which show the heart depolarization and repolarization phases. A short summary on the forms of action potentials as well as the sequence of cardiac activation is shown in Figure 2.6.

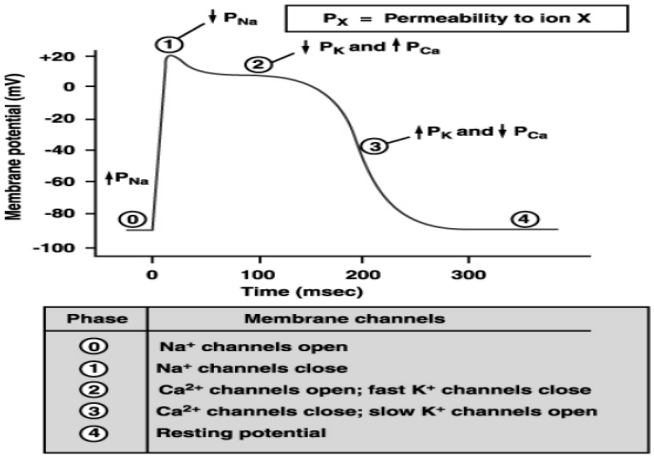

Figure 2.5 Membrane potential changes in heart muscle (polarization-repolarization) [7]

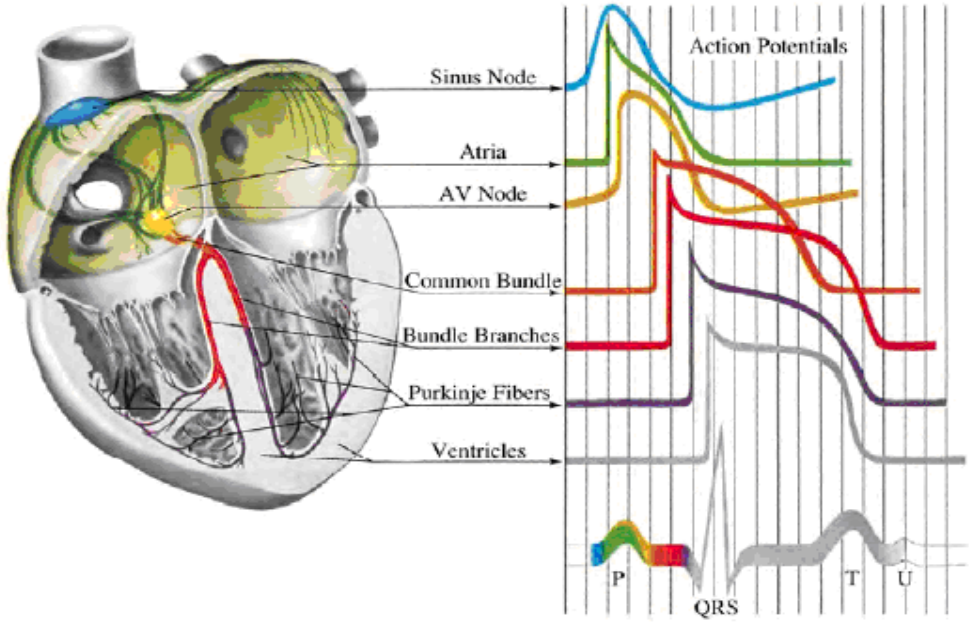

Figure 2.6 The source of ECG wave (summation of action potentials from different tissues of the heart) [7].

CHAPTER 3

FORWARD AND INVERSE PROBLEM OF ELECTROCARDIOGRAPHY

The problem of the ECG can be broken into two distinct problems: the forward problem [8, 9, 10] and the inverse problem [9, 10]. The main interest of inverse and the forward problems of ECG is to explain the connection between electrical activities occuring in the heart and the corresponding body surface potentials. The forward and the inverse ECG problems are illustrated in Figure 3.1.

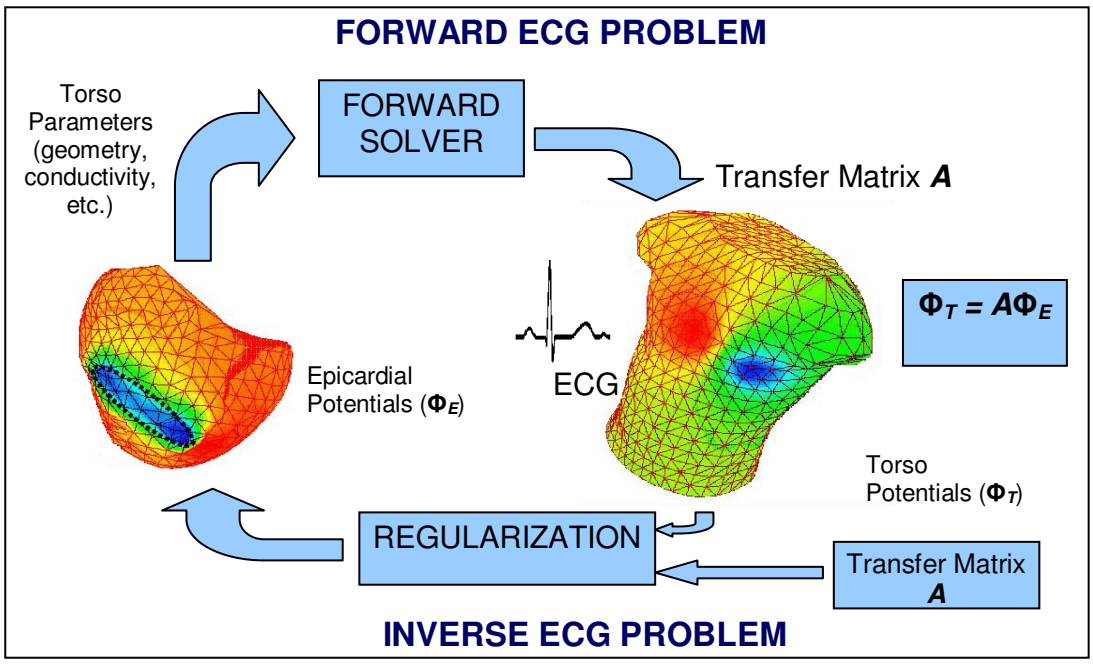

Figure 3.1 Forward and Inverse Problem of the ECG

A forward problem can be defined such kind of problem which seeks to determine the resultant field that is produced from some source. Thus, the forward problem of ECG is used for obtaining the potentials on the body surface that result from a given epicardial source.

The inverse problem of the ECG is a kind of ill-posed problems. Given the resultant body surface potential distribution, the inverse ECG is used for obtaining the epicardial potential distribution. The epicardial potential distribution is obtained non-ivasively in inverse ECG problem. However, due to the tissues in the throax, it is diffucult to obtain the epicardial potentials. Since, these tissues cause smoothing effects of the source cardiac potential until reaching the torso surface. This problem involves lessening the smoothing of the tissues between the heart and torso surface. The difficulty in the problem arises due to its non-uniqueness and ill-posed nature. For the inverse problems, this means that additional constraints have to be introduced into the formulation of the inverse ECG problem in order to reduce the instability of the solution. This instability can be got rid of using a routine, which is called regularization, means that introducing a constraint to the solution to reduce sensitivity contrary to perturbation. The inverse problem is the more useful of the two ECG problems to diagnose the cardiac conditions due to the non-invasive recordings of the electrical activities in practice. It is cheaper and easier to measure epicardial potentials than to measure the potentials invasively.

3.1 Formulation of the Forward Problem

The main aim of the forward problem of the ECG is to compute the body surface potentials (body surface measurements (BSPMs)) [12] (see Appendix B) resultant from a given epicardial potential distribution. The main results of the forward problem are:

- Investigation of the influence of electrophysiological properties (such that geometry, conductivity, etc.) of different tissues on the resulting ECG,
- Optimization of the ECG measurements (such that electrode locations, etc.),
- Computation of the transfer matrix using forward solver (Figure 3.1) for the inverse problem of ECG.

Due to the complicated geometry of the human throax, the direct computation is too diffucult to perform. In order to eliminate this diffuculty, two possible choices can be chosen. First, the geometry can be assumed as a primitive shape (e.g. eccentric spheres model [13]). Discretization of the geometry into homogenous geometry is the other approach to elimate the diffuculty, the forward ECG problem solution methods are employed to solve the problem. The mathematical relation between the epicardial potential distribution and the body surface potential distribution can be defined as follows:

$$A\Phi_E = \Phi_T , \tag{3.1}$$

where $A \in \mathbb{R}^{mxn}$ is the matrix describing the relationship between the epicardial potentials and body surface potentials, with m being the number of body surface electrodes and n representing

the number of epicardial leads; $\Phi_E \in \mathbb{R}^{nxp}$ is the matrix of unknown epicardial potentials and $\Phi_T \in \mathbb{R}^{mxp}$ is the matrix of body surface potentials.

3.2 Inverse Problem

Inverse problems generally consider the reconstruction of the cause by its effects, as opposed to forward problems dealing with the prediction of effects for a known cause. The solution methods for this class of problems are used in many fields of science such as geophysics, optics, image processing, astronomy, etc.. The most common feature of many inverse problems is their ill-posedness, which means that there is no unique solution for this kind of problem. This means that additional constraints have to be used for the formulation of the inverse problem in order to reduce the instability of the inverse problems. This instability can be removed using a procedure, called regularization. Currently, there is a wide usage of the inverse problem to determine the epicardial potential distribution from measured body surface potentials inversely. This problem is called inverse problem of ECG. Posing the problem in terms of reconstructed epicardial potentials, there is a unique determination of the problem, however ill-posedness still exists for the problem. It means that the existance of any perturbation (always exists practically), will be amplified in the solution in an out of control and unknown way. Regularization approaches to the solution of the inverse problem of ECG appeared in the late 60s [14, 15]. Then, in order to find find certain and stable inverse solutions, a particular effort has been shown. At first, much of this effort was spent on researching the effects of different regularization constraints and the regularization parameter choice. It has now been realized that the importance of imposing some form of temporal constraint on the solutions was understood. Since, there are poor performances of algorithms which only regularize in the spatial domain and also the ability to make use of the temporal correlation of solutions at adjacent time steps. Recently, carefully prepared regularization techniques which combine both spatial and temporal constraints on the solutions have been proposed. In this thesis, we ignore the spatial and temporal constraints and solve the inverse problem of ECG at every time instant independently. It is called column sequential solution method. One of the main problems with a regularization technique is that there is no knowledge the regularization degree to apply for solving inverse ECG problem. With a known solution (exact epicardial potential distribution) , it is possible to obtain an optimal regularization parameter which will optimally reconstruct the desired solution. However, exact epicardial potential distribution is not known in practice, so many of the regularization techniques are based on mathematical approaches for ill-posed problems to find regularization parameters.

3.2.1 Formulation of the Inverse Problem

The mathematical relation viewpoint between the epicardial potentials and the body surface potentials was given in (3.1). In the equation, due the ill-conditioned nature of A matrix, small errors during measurement in the BSPMs or existance of geometrical errors in the volume conductor model used in the solution of inverse ECG problem cause large perturbations in the estimation of epicardial distrubitions [16]. This makes it impossible to employ a convential least squares error inverse, defined by the minimization of the residual norm as follows:

$$\min \| A\Phi_E - \Phi_T \|_2 \ , \tag{3.2}$$

where the symbol $\|.\|_2$ is the representation of the Euclidian norm [17]. If A matrix is full-rank, then the solution for 3.1 can be given as follows;

$$\Phi_E = (A^T A)^{-1} A^T \Phi_T \ , \tag{3.3}$$

However, the transfer matrix A is ill-conditioned, therefore the regularization techniques should be used to solve the ill-posed ECG problems in order to lessen the effects of the inevitable perturbation by introducing constraints on the solution.

3.3 Transfer Matrix

A (in equation 3.1) is the transfer matrix between heart and torso that depends on anatomic and electrical properties of heart-torso geometry. The computation of the transfer matrix A is an important and rather time-consuming part of the inverse problem. This matrix contains the information about the conductivity and geometry of the volume conductor. Depending on the choice of equivalent cardiac sources, there exists different approaches to the computation of this matrix. To obtain the transfer matrix A, the well-known Boundary Element Method (BEM) [9,10] is used.

3.4 Regularization Methods

In measured data, the exact body surface potentials, $\Phi_{T_{EXACT}}$, are perturbed by measurement errors. It can be assumed that

$$\Phi_T = \Phi_{T_{EXACT}} + E \ , \tag{3.4}$$

where E represents white Gaussian measurement noise. Due to ill-conditioned nature of the transfer matrix A, the measurement errors cause an amplification on the solution of epicardial potentials, therefore the estimated epicardial potentials will be useless with large errors. So, in order to solve the inverse ECG problem, special techniques (such as regularization methods) are

required. Regularization methods are divided into two groups such that direct regularization methods and iterative regularization methods. Tikhonov, TSVD and TGSVD are examples of direct regularization methods, Least Squares QR Method is an example of iterative regularization methods. The main diffuculty encountered with the problems, which have ill-posed nature ((3.1), (3.2)), is that they are essentially underdetermined due to the particular number of small singular values of A. Hence in order to reduce the instability of the problem, it must be incorporated additional constraints about the estimated solution and to obtain a useful and stable solution. This is the main aim of the regularization. In the following part of this chapter, we give information about the regularization methods which are proposed in literature and their usages to solve the inverse problem of the ECG.

3.4.1 Singular Value Decomposition

Some regularization methods, such as Tikhonov Regularization, TSVD and TGSVD, need singular value decomposition (SVD) to solve inverse problems, therefore we first give a brief summary of SVD before describing the regularization methods. Let us consider the SVD of the mxn transfer matrix A, converting n (lead number) epicardial potentials to m (electrode number) body surface potentials ($m > n$), defined as follows:

$$A = U\Sigma V^T = \sum_{i=1}^{n} u_i \sigma_i v_i^T \ , \tag{3.5}$$

where $U = \{u_1, u_2, ..., u_m\} \in R^{mxm}$ and $V = \{v_1, v_2, ..., v_n\} \in R^{nxn}$, the colums of U and V are orthonormal eigenvectors of AA^T and $A^T A$, respectively, and $\Sigma = diag(\sigma_1, ..., \sigma_n)$ is a diagonal matrix containing the eigenvalues of A. The diagonal terms are ordered in a descending way as follows:

$$\sigma_1 \geq \sigma_2 \geq \ldots \geq \sigma_r > \sigma_{r+1} = ... = \sigma_n = 0, \tag{3.6}$$

where $r = rank(A)$. The σ_i elements are known singular values of A. Using this singular value decomposition of A, the least squares error solution given by (3.1) can be written as follows:

$$\Phi_E = V\Sigma^+ U^T \Phi_T \ , \tag{3.7}$$

where Σ^+ is the psuedoinverse of Σ. The psuedoinverse can be defined as follows:

$$\Sigma^+ = (\Sigma^T \Sigma)^{-1} \Sigma^T \ . \tag{3.8}$$

The matrix Σ^+ is an nxm matrix whose non-diagonal elements are zero and the diagonal elements are given by:

$$\sigma_i^+ = \begin{Bmatrix} \frac{1}{\sigma_i}, & for \sigma_i > 0 \\ 0 \quad , & for \sigma_i = 0 \end{Bmatrix}. \tag{3.9}$$

The pseudoinverse A^+ of the matrix A can be calculated as follows (if A is full rank matrix):

$$A^+ = \sum_{i=1}^{rank(A)} u_i^T \frac{1}{\sigma_i} v_i \ , \tag{3.10}$$

$$\Phi_E = A^+ \Phi_T = \sum_{i=1}^{rank(A)} u_i^T \frac{\Phi_T}{\sigma_i} v_i \tag{3.11}$$

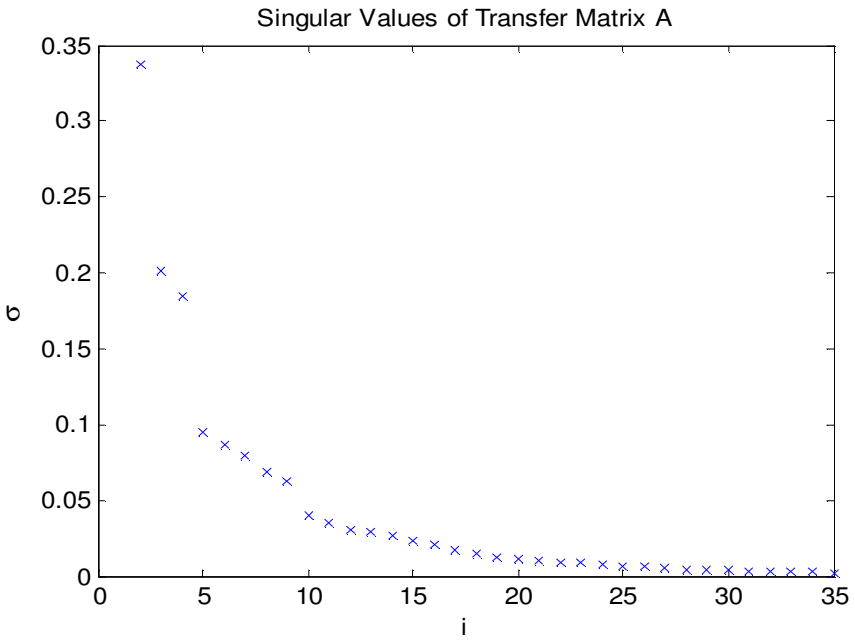

Figure 3.2: Singular values of the transfer matrix A

The singular values (σ_i) of the transfer matrix are usually in a decreasing order (Figure 3.2). The number of zero-crossings of eigenvectors u_i and v_i is growing with increasing i [18, 19]. If there is a measurement error, the solution gets unstable.

3.4.2 Truncated Singular Value Decomposition

Truncated singular value decomposition (TSVD) is a well-known method for solving ill-posed inverse problem. In practise, there exists noise E (geometrical or measurement) on body surface

potential distribution and the matrix A is ill-conditioned, so small singular values of σ_i will magnify the value of the corresponding coefficients $u_i^T E$ in the last summation.

$$A = U\Sigma V^T = \sum_{i=1}^{n} u_i \sigma_i v_i^T \ , \tag{3.12}$$

$$\Phi_{E_{EST}} = \sum_{i=1}^{n} \frac{u_i^T \Phi_{T_{noised}}}{\sigma_i} v_i = \sum_{i=1}^{n} \frac{u_i^T (\Phi_{T_{EXACT}} + E)}{\sigma_i} v_i = \sum_{i=1}^{n} \frac{u_i^T \Phi_{T_{EXACT}}}{\sigma_i} v_i + \sum_{i=1}^{n} \frac{u_i^T E}{\sigma_i} v_i \tag{3.13}$$

The SVD and filter factors are used to eliminate the influence of perturbation in the TSVD regularization for solving inverse ECG problem. The regularized TSVD solution $\Phi_{E_{TSVD}}$ is obtained by first replacing the ill-conditioned matrix A with the rank-k matrix, A_k, defined as follows:

$$A_k = U\Sigma_k V^T = \sum_{i=1}^{k} u_i \sigma_i v_i^T \ , \tag{3.14}$$

which means that small singular values of the treansfer matrix are ignored, since they make the solution unstable . We define filtering factors, f_i, as follows:

$$f_i = \begin{cases} 1 \ , & i \le k \ , \\ 0 \ , & i > k \ , \end{cases} \ , \tag{3.15}$$

where $k \le r = rank(A)$, to eliminate the small singular vaues of the A matrix by this method the noise of the data is eliminated and get the minimized error data. The filtered solution of TSVD is defined by the following equation;

$$\Phi_{E_{TSVD}} = \sum_{i=1}^{n} f_i \frac{u_i^T \Phi_T}{\sigma_i} v_i \ . \tag{3.16}$$

The parameter k is the regularization parameter chosen from regularization parameter finding procedures which will be introduced in the following sections.

3.4.3 Tikhonov Regularization Method

Tikhonov Regularization [20] is the most commonly used method of regularization of ill-posed problems. It introduces a regularization term into the formulation (3.2). The minimization problem can defined as follows:

$$\min \{ \| A\Phi_E - \Phi_T \|_2^2 + \lambda^2 \| L\Phi_E \|_2^2 \ \}, \tag{3.17}$$

where λ is regularization parameter, a positive scalar, that controls the weight given to minimization of the residual norm or solution norm (detailed information in section 3.6). The regularization term $L\Phi_E$ incorporates the a priori information about the solution Φ_E.

There are two important alternative formulations of the problem (3.17):

$$(A^T A + \lambda^2 L^T L) = A^T \Phi_T, \tag{3.18}$$

$$\Phi_{E\lambda} = \arg\min_{\Phi_E} \| \begin{pmatrix} A \\ \lambda L \end{pmatrix} \Phi_E - \begin{pmatrix} \Phi_T \\ 0 \end{pmatrix} \|_2 \tag{3.19}$$

Thus, if there is an intersection between the null spaces of A and L matrix trivially such as the coefficient matrix has a full rank property, then there is a unique Tikhonov solution, and it can be given as follows;

$$\Phi_{E_{TIKJHONOV}} = (A^T A + \lambda^2 L^T L)^{-1} A^T \Phi_T . \tag{3.20}$$

If matrix L is the identity matrix $(L = I)$, the method is referred to as Tikhonov 0-order, else if L is a surface gradient operator, then the method is the first order regularization and for second order regularization L is a surface Laplacian operator. In terms of TSVD, the Tikhonov regularization is equivalent to the introduction of filtering factors into (3.11), reducing the effects of the high-frequency components of the solution:

$$f_i(\lambda) = \frac{\sigma_i^2}{\sigma_i^2 + \lambda^2},\ L = I \quad and \quad f_i(\lambda) = \frac{\gamma_i^2}{\gamma_i^2 + \lambda^2},\ L \neq I, \tag{3.21}$$

where filter factors are used for ignoring the small singular values, in this case, the filter factors are defined for the Tikhonov regularization method.

$$\begin{aligned} \Phi_{E_{TIKHONOV}} &= \sum_{i=1}^{n} \frac{\sigma_i \mu_i^T \Phi_T}{\sigma_i^2 + \lambda^2} \upsilon_i = \sum_{i=1}^{n} \frac{\sigma_i^2}{\sigma_i^2 + \lambda^2} \frac{\mu_i^T \Phi_T}{\sigma_i} \upsilon_i, \\ &= \sum_{i=1}^{n} f_i \frac{\mu_i^T \Phi_T}{\sigma_i} \upsilon_i . \end{aligned} \tag{3.22}$$

3.4.4 Least Squares QR Method

The least squares QR (LSQR) method is one of the iterative regularization method based on Lanczos bidiagonalization (LBD) [21, 22] and QR Factorization [23]. The LSQR method is more efficient than the well-known conventional regularization methods such that Tikhonov and

TSVD which require SVD procedure, which is an expensive operation in computationally when the transfer matrix A has a large dimension and ill-conditioned nature. The run-time costs of two decomposition methods are given in Table 3.1.

Table 3.1 The run-time costs of two decomposition methods.

Method	Time (seconds)
SVD	2.48
QR	0.79

Due to iterative properties of LSQR method, we need a stopping point to finalize the iteration. The k th matrix $\Phi_E^{(k)}$ is the regularization solution (optimal) which is obtained after k iterations. If iteration of the regularization is not stopped, this method may converge to noise corrupted worse solution with a high relative error (RE). Consider the matrix $A \in \mathbb{R}^{m \times n}$, the LBD computes the factorizations. Vectors, $\mu_j \in \mathbb{R}^m$, $v_j \in \mathbb{R}^n$ and scalars α_j and β_j, which meets $U^T AV = B_k$. We choose an iteration number k, and then the method computes three matrices, a lower bidiagonal matrix B_k and two matrices U_{k+1} and V_k related by

$$\Phi_T = \beta_1 \mu_1 = \beta_1 U_{k+1} e_1, \tag{3.23}$$

$$AV_k = U_{k+1} B_k, \tag{3.24}$$

$$A^T U_{k+1} = V_k B_k{}^T + \alpha_{k+1} v_{k+1} e_{k+1}^T. \tag{3.25}$$

Here, the bases $U_{k+1} \in \mathbb{R}^{m(k+1)}$ and $V_k \in \mathbb{R}^{mxk}$ have orthonormal columns, e_i is the unit vector and the matrix $B_k \in \mathbb{R}^{(k+1)xk}$ is lower bidiagonal:

$$B_k = \begin{bmatrix} \alpha_1 & & & 0 \\ \beta_2 & \alpha_2 & & \\ & \beta_3 & \ddots & \\ & & \ddots & \alpha_k \\ 0 & & & \beta_{k+1} \end{bmatrix}, \tag{3.26}$$

$U_{k+1} = (u_1, u_2, u_3, ..., u_{k+1}) \in \mathbb{R}^{mx(k+1)}$, $U_{k+1}^T U_{k+1} = I_{k+1}$, $V_k = (v_1, v_2, v_3, ..., v_k) \in \mathbb{R}^{mxk}$ and $V_k^T V_k = I_k$.

$$\Phi_E^{(k)} = v_k y^{(k)}, \tag{3.27}$$

$$r^{(k)} = \Phi_T - A\Phi_E^{(k)}, \tag{3.28}$$

$$r^{(k)} = \beta_1 u_1 - AV_k y^{(k)} = U_{k+1}(\beta_1 e_1 - \beta_k y^{(k)}), \tag{3.29}$$

$$t_{k+1} = \beta_1 e_1 - B_k y^{(k)}, \tag{3.30}$$

$$Q_k \begin{bmatrix} B_k & \beta_1 e_1 \end{bmatrix} = \begin{bmatrix} R_k & f_k \\ & \phi_{k+1} \end{bmatrix}, \tag{3.31}$$

$$\Phi_E^{(k)} = v_k y^{(k)}, \quad R_k y_k = f_k, \tag{3.32}$$

$$\Phi_E^{(k)} = v_k R_k^{-1} f_k. \tag{3.33}$$

The iteration stopping point is calculated by the L-curve method, using norm of each iteration solution $\| \Phi_E^{(k)} \|_2$, on the ordinate versus the norm of residual $\| A\Phi_E^{(k)} - \Phi_T \|_2$ on the abscissa, with k as a parameter which is located corner of the resulting curve generally.

3.4.5 Bayesian Maximum a Posteriori (MAP) Estimation

The regularization method of Bayesian MAP employs a statistical basis of a priori estimations of the inverse problem solutions, and chooses the best solution fitting the given observation $\Phi_{T_{NOISED}}$ out of it. This approach is based on the theory developed by Foster [24].

The problem in (3.4) can be expressed as follows:

$$\Phi_T = A\Phi_{E_{EXACT}} + E, \tag{3.34}$$

where E is random measurement errors, assumed to have exact and zero mean covariances [25]. The goal is to construct a matrix operator $\Gamma \in \mathbb{R}^{n \times m}$ such that the averages

$$\Phi_{E_{EST}} = \Gamma \Phi_T \tag{3.35}$$

is the solution of (3.34). Combining (3.34) and (3.35) we obtain:

$$\Phi_{E_{EST}} = \Gamma A \Phi_{E_{EXACT}} + \Gamma E. \tag{3.36}$$

Let's represent $R = \Gamma A$ then (3.36) can be represented as follows:

$$\Phi_{E_{EST}} = R\Phi_{E_{EXACT}} + \Gamma E, \tag{3.37}$$

where the rows of R matrix represent a set of filters transforming the exact solution $\Phi_{E_{EXACT}}$ to our estimation $\Phi_{E_{EST}}$ minus some random errors. If the exact solution $\Phi_{E_{EXACT}}$ is subtracted from both sides of equation (3.35), the estimation error can be obtained:

$$\Phi_{E_{EST}} - \Phi_{E_{EXACT}} = (\Gamma A - I)\Phi_{E_{EXACT}} + \Gamma E \tag{3.38}$$

The first summation at the right side of (3.38) is generally defined as a resolving error, whereas the the other term referred to random error. If $\Phi_{E_{EST}}$ provides a reasonable estimation of $\Phi_{E_{EXACT}}$, both of these terms must be small. For the variability of $\Phi_{E_{EXACT}}$, a statistical description is given, can be defined in the form of covariance matrix C_x, and the errors in an estimation may be assumed as independent in statistically on the data errors E, the estimation errors of the covariance $\Phi_{E_{EST}} - \Phi_{E_{EXACT}}$ can be defined as follows:

$$C = (\Gamma A - I)C_x(\Gamma A - I)^T + \Gamma C_e \Gamma^T \ . \tag{3.39}$$

The first summation on the right is the resolving errors for the covariance, the second term on the right defines the random errors of the covariance. The estimator which minimizes the diagonal elements C in (3.39) is

$$\Gamma = C_x A^T (A C_x A^T + C_e)^{-1} \ , \tag{3.40}$$

which is widely known as the minimal variance estimator. This equation was originally derived in [26] as linear estimator which is the best when Φ_E is a production of a second-order random process of Gaussian. The distribution of Gaussian assumption is still not needed, the estimation errors variance can be minimized by (3.40) no consideration of the form of a probability density of Φ_E. In this way an estimate of Φ_E can be obtained by as follows:

$$\Phi_{E_{EST}} = C_x A^T (A C_x A^T + C_e)^{-1} \Phi_T \ , \tag{3.41}$$

which is used as the solution of the inverse problem. A new methodology was introduced recently which was based on the Bayesian MAP estimation to solve the inverse problem of ECG [27, 28].

3.5 Choice of Regularization Parameter

Regularization parameter, a positive scalar, balances the tendency given to minimization of the solution norm versus minimization of the residual norm. It is represented by the symbol λ or k generally, according to the regularization methods. An optimum regularization parameter should supply a fair balance between the regularization error and the perturbation error in the solution of regularization. If λ is chosen to be too small, the high frequency components of (3.11) might be selected, carrying no useful information about the cardiac sources. This is called under-regularization. Also, if λ is choosen too large, the useful high-frequency components of the signals can be suppressed. It causes a smoothing effect on the solution, it is called as over-regularization.

Thus selection of the optimum regularization parameter is extremely important for the solution of the inverse problem of ECG. In Literature, several methods were suggested to find the optimal value of λ such as L-curve, composite residual and smoothing operator (CRESO), optimal criterion and generalized cross validation (GCV).

3.5.1 L-curve

The L-curve is well-known method which is used to determine the optimal value of regularization parameter after the works of Hansen [29, 30]. In terms of the Tikhonov regularization, the L-curve is a parametric plot with points defined by the norm of the residual $\| A\Phi_{E\lambda} - \Phi_T \|_2$ and the norm of the regularization term $\| L\Phi_{E_\lambda} \|_2$ for different values of the regularization parameter λ:

$$\| L\Phi_{E\lambda} \|_2 = f(\| A\Phi_{E\lambda} - \Phi_T \|_2) \quad (3.42)$$

This plot is usually built for λ changing within the range between the minimal and maximal eigenvalues of A. A typical L-curve for the case of measured signals $\Phi_{T_{EST}}$ corrupted with noise is shown in Figure 3.3.

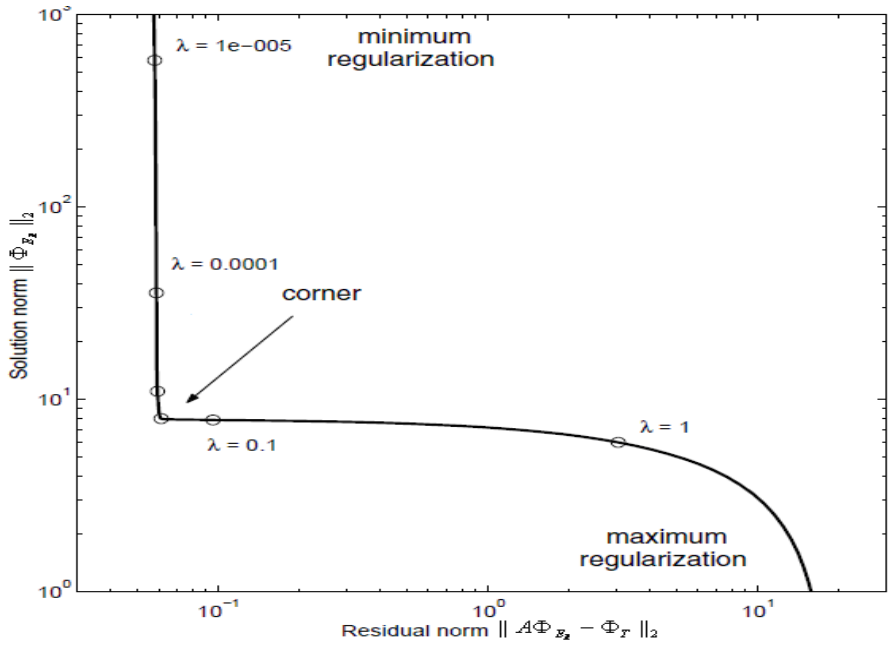

Figure 3.3: Sample L-curves resulting from the solution of a typical inverse problem of the ECG [31].

The optimal value of λ is found at the point of the maximal curvature of the L-curve, where its second derivative has its maximum. This point is referred to the corner of the curve. Moving the chosen λ along the curve towards the significant increase of the residual norm leads to over-regularization, whereas the movement of λ towards the increasing $\| \Phi_E \|_2$ leads to under-regularization of the solution [31].

3.5.2 Creso

The composite residual and smoothing opeartor (CRESO) [29] is the other well-known method for choosing regularization parameter. In Figure 3.4, we see a sample CRESO curve. The CRESO method depends on the localization of the maximum of the following function:

$$C(\lambda) = \| \Phi_{E\lambda} \|_2^2 + 2\lambda^2 \frac{d}{d(\lambda^2)} \| \Phi_{E\lambda} \|_2^2 \tag{3.43}$$

If the SVD of A matrix is known, then the computation of C(λ) can be done as follows:

$$C(\lambda) = \sum_{i=1}^{rank(A)} \left(\frac{\sigma_i}{\sigma_i^2 + \lambda^2} u_i^T \Phi_T \right)^2 \cdot \left(1 - \frac{4\lambda^2}{\sigma_i^2 + \lambda^2} \right) \tag{3.44}$$

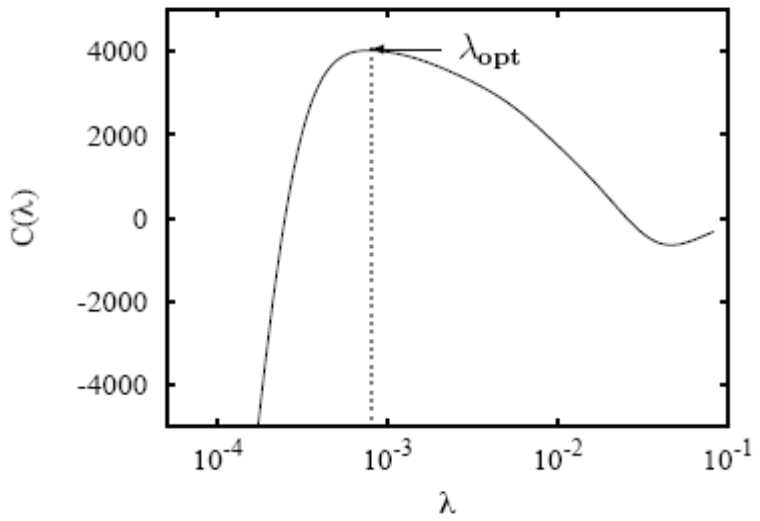

Figure 3.4 A sample CRESO curve [32].

3.5.3 Optimal Criterion

The optimal regularization parameter [29] is obtained by estimating epicardial potentials which minimizes the RE compared to the known epicardial potentials. The value of optimal criterion can be defined as:

$$RE = \frac{\| \Phi_{E_{EST}} - \Phi_{E_{EXACT}} \|}{\| \Phi_{E_{EXACT}} \|}, \tag{3.45}$$

where $\Phi_{E_{EXACT}}$ denotes the known epicardial potential distribution and $\Phi_{E_{EST}}$ stands for the computed one.

3.5.4 Generalized Cross Validation

Generalized Cross Validation (GCV) [29] is based on the principle that if any arbitrary element is left out, then the corresponding regularized solution should predict this observation. Then, it yields for choosing a regularization parameter which minimizes the GCV function

$$G = \frac{\| A\Phi_{E_{EST}} - \Phi_T \|^2}{(trace(I - AA^I))^2}, \tag{3.46}$$

where A^I is the matrix which produces the regularized solution $\Phi_{E_{EST}}$ when multiplied by Φ_T. In the calculation of the cross validation method, there is a major diffuculty due to the calculation of the inverse matrix trace.

CHAPTER 4

CONTRIBUTIONS OF GENETIC ALGORITHMS FOR SOLVING INVERSE PROBLEM OF ELECTROCARDIOGRAPHY

4.1 Genetic Algorithms

Genetic algorithms (Gas) are stochastic search techniques used to find solutions to optimization problems which are quite hard to solve by conventional methods. Genetic algorithms are a particular class of evolutionary algorithms which are based on the simulation of natural evolutionary process of human beings. The working processes of evolution suit well for some of the huge computational problems for many fields. These problems require searching through a huge number of possible solutions. The rules depend on the natural selection in evolutionary computation [33]. The solutions vary due to the GA operators such that crossover or mutation. Cells are the basic structures of all living organisms, and they contain one or more small structures called chromosomes. The chromosomes can be defined as DNA strings [33]. These structures are used for the identification of the living organism. A chromosome is a squence of genes. The genes can be exprerssed as a definition for a property, like hair, eye colour, etc. For the natural selection fitness functionality is the other important concept for a living organism [33, 34]. The probability of the survival of the organism is the defitinon of the fitness functionality. The fittest indivual has the biggest chance to survive.

In order to start the GA process, a randomly initialized population is selected, then a probabilistic, parallel search in the solution space are performed to form a new population of candidate solutions. The population undergoes a simulated evolution process. At each generation the fittest solutions are reproduced, while the other solutions are ignored. In the end, the last generation has the fittest chromosomes through all generations. The conceptual algorithm of the GA is shown in Figure 4.1.

4.2 Genetic Algorithm Operators

Three basic GA operations are performed on these chromosomes of the current generation to produce child generations that become fitter in the simulated evolution process. These three basic

operations are selection, crossover, mutation [33, 34, 35] (Figure 4.1, 4.2). The GA operators are explanied in the following sections. (the subtitles of these operators are explained in details in Appendix C).

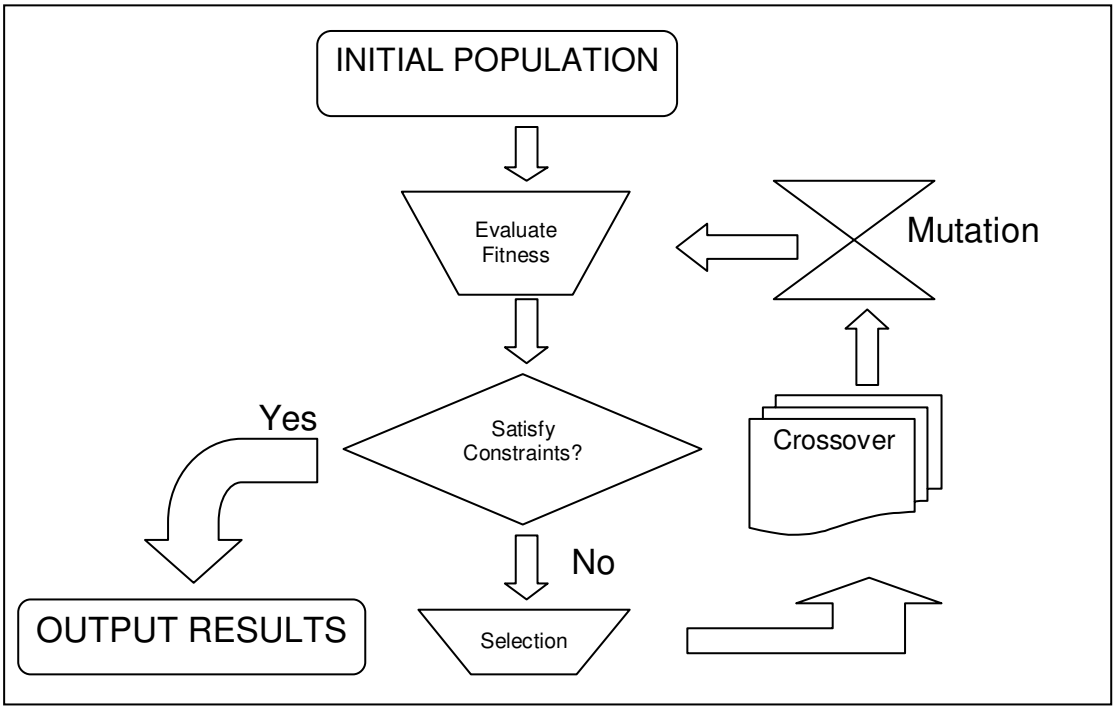

Figure 4.1 – The GA Work Flow

- **Selection**

The selection operation has several similarities with the Darwin's natural selection process which is explained as evolution theory [33]. During the selection process, a group of chromosomes from the current generation is chosen for reproduction. This selection is based on the fitness values of the chromosomes of the population and improvement of the average quality of the population is the aim of this operation. Due to the selection process, the individuals of higher fitness will have a higher probability of being copied their characteristics to produce new individuals of the next generation. Since the selection depends on the fitness value of the individuals.

- **Crossover**

Once the chromosomes are selected, new chromosomes of the child generation are formed using the crossover operation. Crossover is one of the most important operation in GA. It merges two chromosomes from current generation to create two offspring for the child generation. Individuals from current generation are picked in pairs from the selected chromosomes to

become parents with a specified ratio of crossover probability. By this operation new born chromosomes (childs) carry on their characteristics of parents according to the probability value.

- **Mutation**

The mutation operator modifies a chromosome in current generation. The main goal of the operator is to hinder the GA population from converging to a local minimum and to put some new candidate solutions to the population. It yields a variety in the current generation. One of the properties (gene values) of a chromosome is changed during the mutation process with a specified probability. The probability of mutation is generally chosen to be very small. Otherwise, the big rate of the mutation probability tends to destroy valuable information which is important for the chromosomes to have higher fitting value. The crossover and mutation rate are determined in an experimental way. This operation provides maintaining variety in the population by pushing the algorithm searching in different regions of the decision place. Applying the GA operations (selection, crossover and mutation) repeatedly, the IP is translated into new populations in an iterative manner, which will tend to contain better individuals and will generally converge to an optimal population.

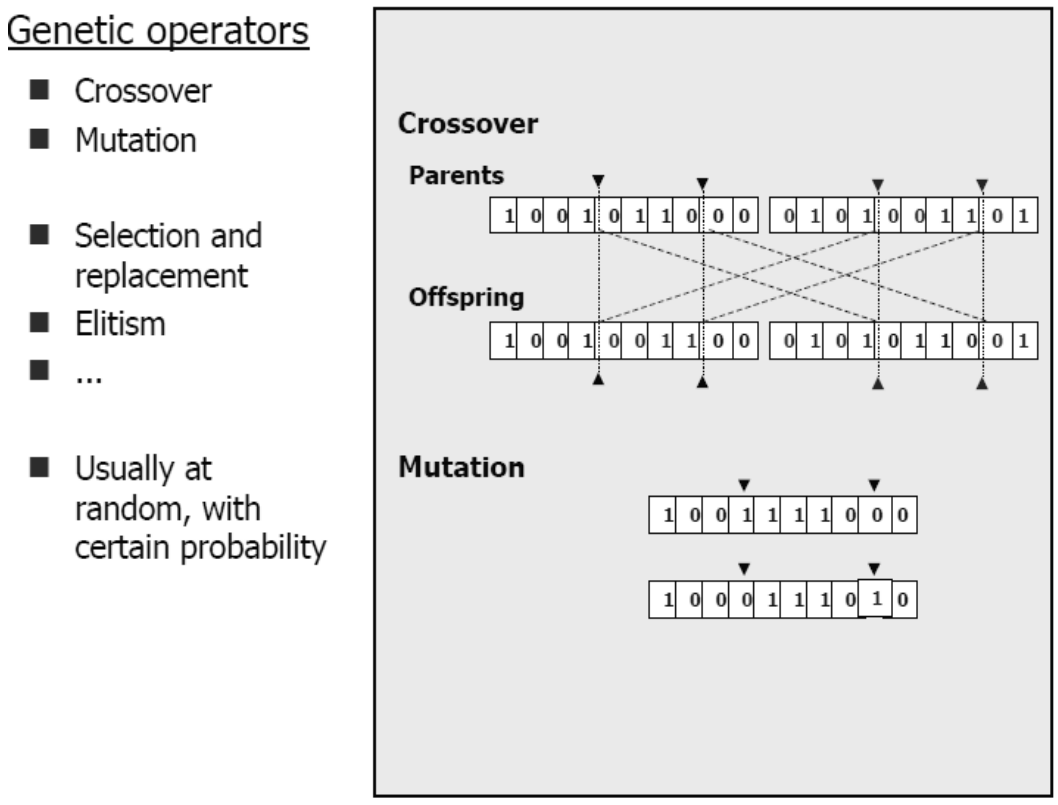

Figure 4.2 The GA Operators [35]

4.3 Combination of GA and Regularization Methods in Literature

Due to the big rate of death, caused by the heart illnesses, many researches have been done to learn about the electrical activity of the heart. Obtaning epicardial potential distribution is a key point to learn the defects of the heart without invasive operation. Computation of epicardial potential distribution without invasive operation is a diffucult process since the electrical signal looses some properties in throax until reaching the body surface. However, the regularization methods, commonly known in literature, provide us with estimation of epicardial potentials from body surface potential distribution. The conventional regularization methods reconstruct epicardial potentials from body surface potentials by smoothing or truncating the noise. Recently, the stochastic search technique, called the GA, is combined with regularization methods to solve the inverse ECG problem. Tikhonov Regularization Method and LSQR method were combined with GA in literature [36, 37]. According to the results proposed, GAs can improve the regularization of inverse ECG problem when combined with regularization methods or additional constraints about solutions. The GA is an efficient optimization technique for improving the solution of the ill-posed inverse ECG problems.

4.4 New Approaches to the Usage of GA for Solving the Inverse Problem of ECG

In this study, we employed several regularization methods to reconstruct the epicardial potentials from the simulated noisy torso potentials. We used the regularized epicardial potentials to employ the GA to improve the regularization. The regularization methods' solutions were used as the additional information to construct the IPs for GA. Addition to literature studies, we combined two other regularization methods, such as TSVD and Bayesian MAP Estimation, with GA. In order to optimize the estimated epicardial potentials by applying GAs, we considered float number encoding GA which used selection (roulette selection, tournament selection, etc.), crossover (scattered, custom, etc.), mutation (Uniform, Gaussian, etc.) and elitist selection. To run the regularization methods, regularization parameter obtaning methods, GA parameters and the comparison of the results, we have implemented a graphical user interface which is explained in Appendix A.

The GA operators and the parameters used for the GAs can be chosen from the GUI as follows:

- Population size npop = N ,
- Crossover type, crossover rate $cr = C_r$,

- Selection such as, Tournament selection where tournament size $k = K$, tournament probability as $pt = P_t$,
- Mutation such as, Uniform mutation where mutation rate $m_r = P_m$,
- Elitism, number of elitist chromosome chosen without applying any GA operations $ne = N_E$.

By using the GA operators and the parameters listed above, the new offspring is produced from the current population. Next, the current population and the newly produced children population are merged and N individuals are selected using one of the selection types (see Appendix C) to obtain the next generation. The inverse ECG problem which is the form of (3.1) considered in this thesis were reformulated as a problem of optimization by minimizing the fitness function, such as the formulation of (3.2). The generation number for a typical GA is in the range 50-300, but more generations can be required. Discrepancy principle is a kind of process to determine the number of generations required [36]. The individuals of the initial population are generated randomly. Therefore, in the early stages of the GA process the global optimum of the problem was unstable and non-converging solution could appear in the population. It causes the GA to be stationary from optimum point of the problem. However, the regularized solution is not the optimum of the object function for ill-posed problems but a solution to fullfill the balance between the fitting and smoothness to the data. Therefore, if additional constraints to the solution of the inverse ECG problem were available, then the constraints should be added to the GA phase to avoid unstable solutions. Afterwards, the GA could be successfully applied to find the global optimum of the inverse ECG problem and would get good solution with low RE and high CC.

4.4.1 Theory

In addition to the literature, we proposed two new approcaches to optimize the epicardial potential distribution.

1. Several regularization methods solved the inverse ECG problem by using additional constraints like regularization parameter. The L-curve is the well-known method to obtain the regularization parameter. Generally, the corner of the L-curve is the optimum regularization parameter. If we apply this parameter to the regularization methods we expect the optimum value of epicardial potentials and it is true in practice. However, the pretty localized potential features are lost because of the smoothing or truncating effects of the regularization methods. In this case, we did experiments to solve the regularization method not only for the optimum value of regularization parameter but for the regularization parameters around the optimum regularization parameter. By this way,

we obtained optimum, under- and over-regularized epicardial potentials. These potentials were the IP for GA. Then the GA started to process to optimize these epicardial potentials. We proposed that the GA could recover the some good properties of the epicardial potentials which are lost when solving by using only the optimum λ and the regularization methods.

2. We had a training set which had eight different epicardial potentials. They were measured from a dog heart. We bypassed the "regularization by using regularization methods" part and applied GA to the training set directly to see whether the GA could improve to regularize the epicardial potentials. According to the results (in Chapter 5) the GA could succeed to optimize the training set and gave us improved epicardial potentials.

In both cases we used the form (3.2) as the fitness function to fit the chromosomes in the GA phase. The results showed that there was a decrease in RE and an increase in the CC compared to the other solution methods. The GA also contributed to the optimization of reconstructed epicardial potentials which were obtained from conventional regularization methods.

CHAPTER 5

RESULTS AND DISCUSSIONS

In this thesis, we used simulated torso potential measurements to test our solution approaches. The epicardial potentials used to simulate the torso potential measurements in this study have been recorded by Dr. Robert S. MacLeod and his coworkers at the University of Utah, Nora Eccles Harrison Cardiovascular Research and Training Institute (CVRTI) from a dog heart that was placed in a realistic torso tank [38].

In these simulations, epicardial potential measurements from 490 points were used and the torso potential measurements were simulated at 771 points. In general torso potential distributions include measurement noise. These noisy torso potentials were obtained by multiplying the epicardial potentials by a transfer matrix obtained from a realistic human torso model using the BEM, and adding white Gaussian noise: the noise level is defined by the input parameter in decibels (dB) (Figure 5.1).

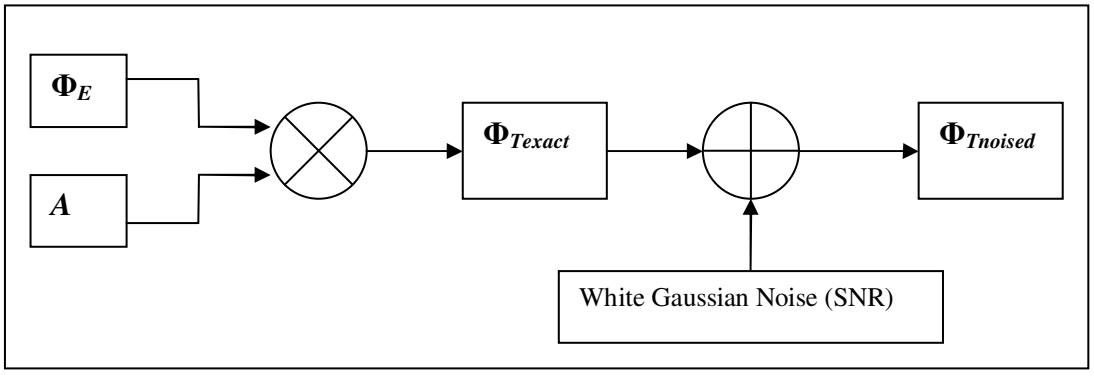

Figure 5.1 Obtaining noisy torso potentials

In our simulations, we added 30 dB Gaussian noise to the calculated torso potentials to simulate the real life cases. Thus, we had:

$$\Phi_T = \Phi_{T_{EXACT}} + E \ , \tag{5.1}$$

where $\Phi_T \in \mathbb{R}^{771x97}$ was the matrix of torso potential measurements, $E \in \mathbb{R}^{771x97}$ was the matrix which stands for the noise and $\Phi_E \in \mathbb{R}^{490x97}$ was the unknown epicardial potential matrix. Each column in these matrices corresponded to a single time instant. Each row of Φ_E corresponded to a node on the heart, whereas each row of Φ_T and E correspond to a node on the body surface. At each time t the epicaridal potential was found at that time. In that case the equation (5.1) above became as follows:

$$\Phi_T(t) = A\Phi_E(t) + E(t) \,, \tag{5.2}$$

so $\Phi_T(t) \in \mathbb{R}^{771x1}$, $E(t) \in \mathbb{R}^{771x1}$, $A \in \mathbb{R}^{771x490}$.

We display the measured epicardial, and calculated torso potential distributions respectively at three different time instants, using a visualization software called the Map3d [39] in Figure 5.2 and Figure 5.3. Note that the lungs were removed from the model to calculate the transfer matrix used in the inverse solution.

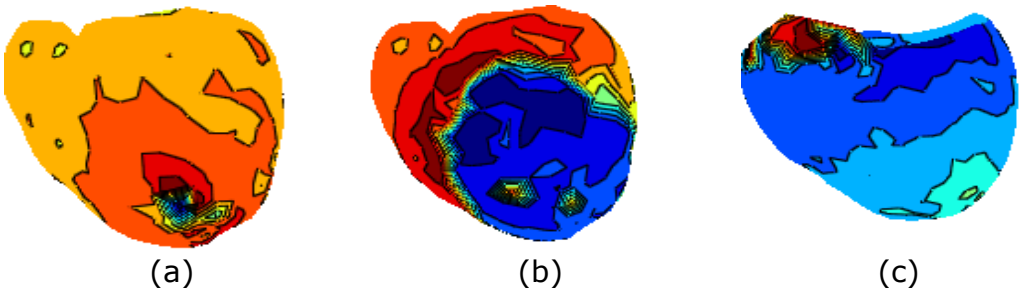

Figure 5.2 The map3d visualization of data of the original epicardial potentials. a) 1st time instant, b) 68th time instant, c) the last time (97th) instant.

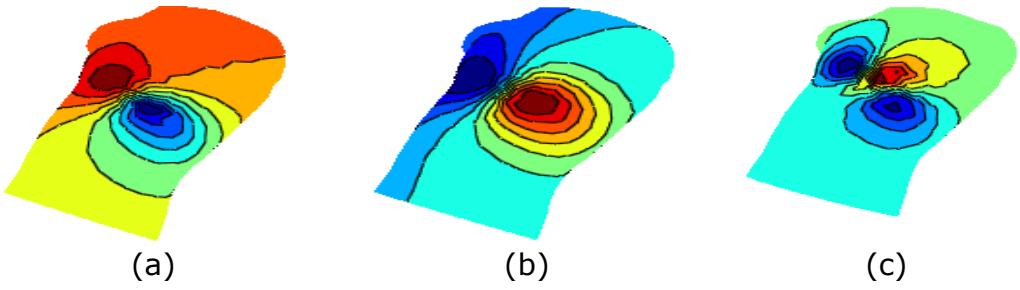

Figure 5.3 The map3d visualization of the torso potentials calculated from measured epicardial potentials. a) 1st time, b) 68th time, c) the last time (97th) instant.

5.1 Simulations

We applied the conventional regularization methods to solve ill-posed ECG problem and combined the regularization methods with the GA. We got improved regularized epicardial potentials with low RE. In this section of this thesis, we give the solution of the inverse problem of ECG using the following approaches:

1. Single Tikhonov Regularization Method,
2. Single TSVD Method,
3. Single LSQR Method,
4. Single Bayesian MAP Estimation Method,
5. Combination of the GA with

    - Tikhonov Regularization Method,
    - TSVD Method,
    - LSQR Method,
    - Bayesian MAP Estimation Method.

6. Apply the GA to an IP which consisted of eight epicardial potentials (training set). In this study, test and training data are different QRS beats obtained from the same heart, but the initial stimulus sites are different for all beats; the stimulus sites of the training set beats are within the second-order neighborhood of the test beat stimulus site,
7. Apply the GA to an IP which consists of a mixture of optimum, over- and under-regularized Tikhonov Regularization solutions.

We used the L-curve and the GCV to obtain the regularization parameter for Tikhonov regularization, TSVD and the LSQR methods. In Bayesian MAP estimation, the covariance matrix was obtained by using the training set. The solution procedure of the conventional regularization methods for inverse ECG problem is given in Figure 5.4.

Figure 5.5 summarizes the solution of inverse problem of ECG with the combination of regularization methods and the GA. In this approach, first, we simulated noisy torso potential measurements by adding white Gaussian noise vectors with different seeds to the exact torso potentials (calculated from the multiplication of transfer matrix and the known epicardial potentials) in order to obtain simulated torso potentials. This gave us many realizations of torso potential measurements corresponding to the same source distribution. Then we applied the conventional regularization methods to reconstruct noise eliminated epicardial potentials.

These estimated epicardial potentials corresponding to *n* different realizations of the same noise-free torso potential measurements are then used as the IP for the GA process. After finishing regularization step, the GA phase started. In this case there was a fitness function to decide whether newly produced chromosomes, fit the data or not. We defined fitness function in two ways. If we know the exact epicardial potentials then the RE (5.3) can be used as a fitness function. However, in clinical applications, the epicardial potentials are not known. Therefore, we used the expression in equation 3.2 as an alternative fitness function. In both cases, the solutions that yield the lowest values of the fitness functions are passed to the next generation. Then in GA phase, we calculated the torso potentials from optimized epicardial potentials to compare the simulated torso potentials. We tried to fit the potential values. We employed all regularization methods mentioned in this thesis, then we combined them with the GA. We implemented a graphical user interface (see Appendix A) to run all of the cases and got the regularization and the GA results. The GA is an iterative algorithm and it requires a stopping criteria. In our study, we used three stopping criteria as follows;

a. RE value,
b. Maximum iteration number,
c. After each iteration, searching whether the GA continues to improve to get better results over a specified value according to the previous generations, if not stop iteration.

Finally, we compared the results of GA and the regularization methods to decide whether the GA contributed to improve the regularization of the epicardial potentials.

There are four criteria to compare the reconstructed epicardial potential results. These are:

- Relative Error,
- Correlation Coefficient,
- Root Mean Square (RMS) Error
- Map3d visualization:

$$RE(t) = \frac{\| (\Phi_{EST})_t - (\Phi_E)_t \|_2}{\| (\Phi_E)_t \|_2}, \tag{5.3}$$

$$CC(t) = \frac{\sum_{t=1}^{n} \left[(\Phi_{EST})_t - (\bar{\Phi}_{EST})_t \right] . \left[(\Phi_E)_t - (\bar{\Phi}_E)_t \right]}{\| \Phi_{EST} - \bar{\Phi}_{EST} \|_2 . \| \Phi_E - \bar{\Phi}_E \|_2}, \tag{5.4}$$

$$RMS(t) = \frac{\| (\Phi_{EST})_t - (\Phi_E)_t \|_2}{\sqrt{length((\Phi_E)_t)}}, \tag{5.5}$$

where t denotes the time instant, Φ_E denotes the known epicardial distribution, and Φ_{EST} the computed one. The quantities $\bar{\Phi}$ and $\bar{\Phi}_{EST}$ are respectively the mean values of Φ_E and Φ_{EST} over the epicardial sites.

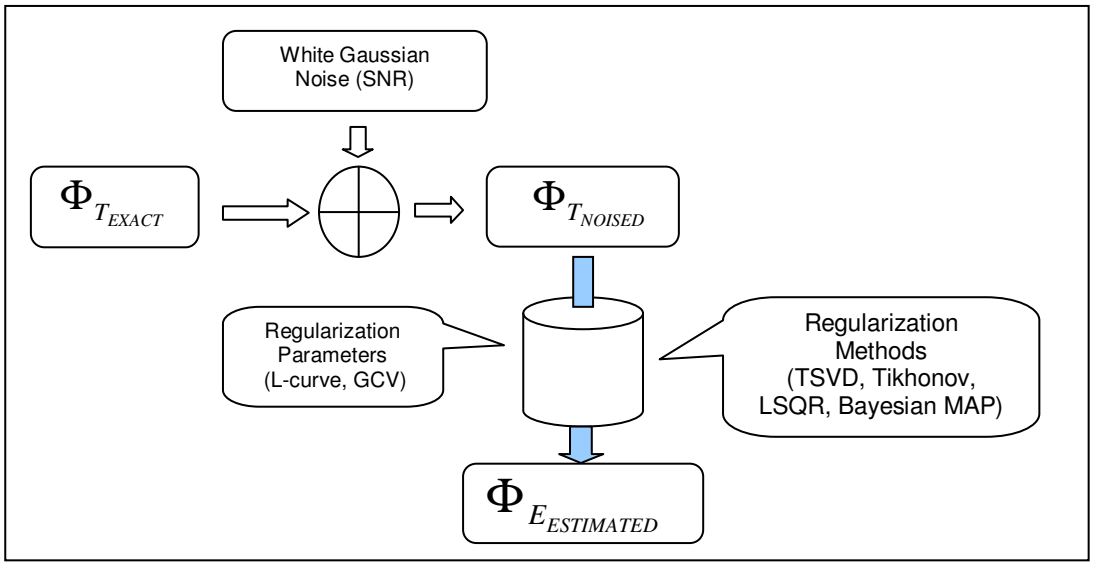

Figure 5.4 Solution phases of the conventional regularization methods for solving inverse ECG problem

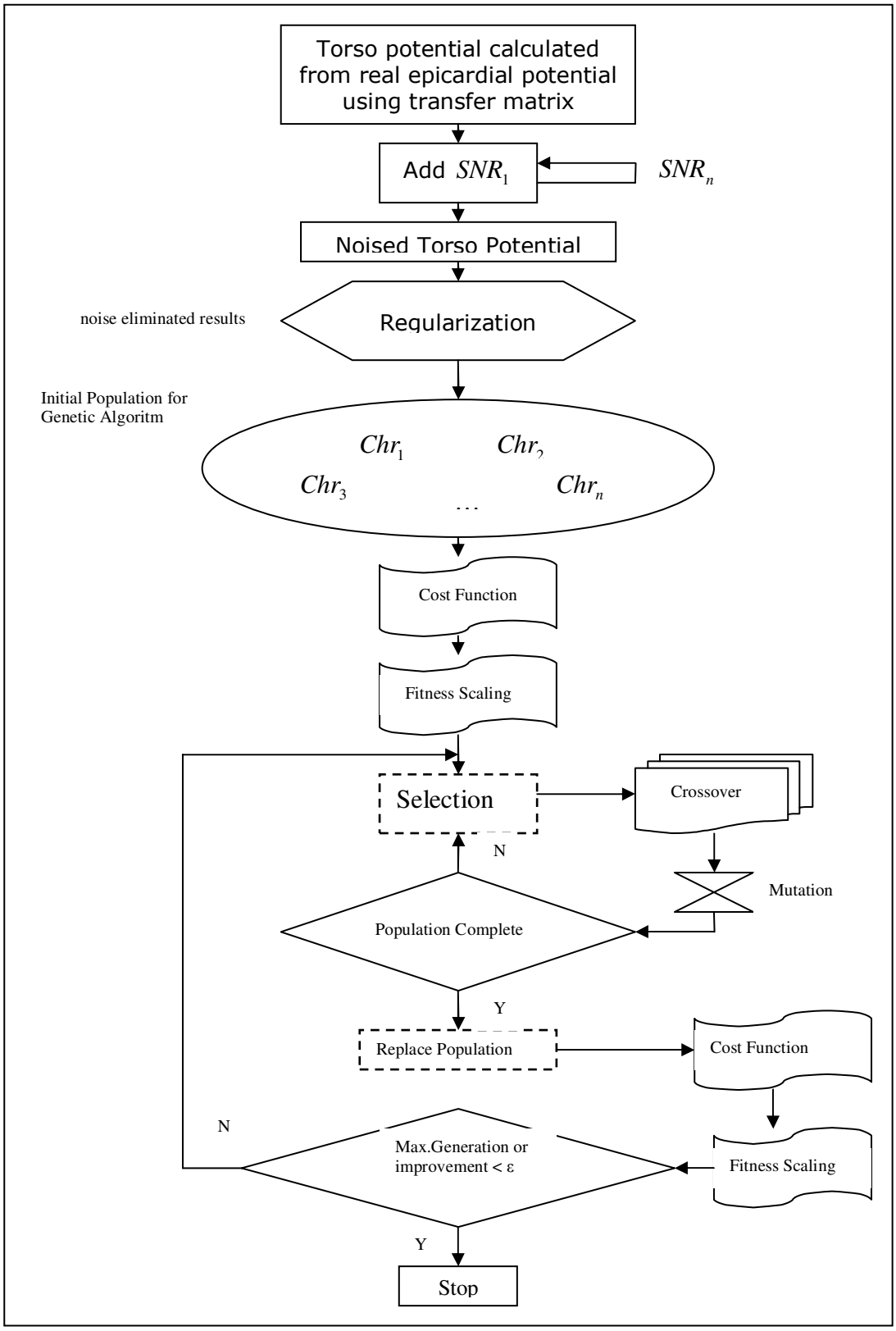

Figure 5.5 Solution for Inverse problem of ECG using combination of regularization methods with genetic algoritm, *n*: number of SNR values with different seeds (chromosome count in population), "ε": improvement rate

5.2 Results

In this section, we give comparison results of our study. In section 5.3.1, we give the results of conventional regularization methods which chooses regularization parameter from L-curve and GCV seperately. We plot the L-curve and GCV graphs for each case. Then we compare the results using the visualiation tool Map3d, RE, CC and RMS Error. In section 5.3.2, we give the results of combination of regularization methods with the GA. Each regularization methods are combined with the GA then the results of each combination are compared among themselves. The results of the GA combined regularization methods are also compared in section 5.3.2.5 to decide which methods respond to GA rapidly and improve the regularization results effectively. Also, in seciton 5.3.2.6 we applied GA directly to the training set of epicardial potentials. We compare the results of Bayesian MAP Estimation and Tikhonov Regularization Methods. We solved Tikhonov Regularization by using not only optimum regularization parameter but also, a range from under-regularized to over-regularized regularization parameter values. We compare the results of the GA combined results of Tikhonov Regularization method uses these λ ranges in section 5.3.2.7. In 3D surface plots with the Map3d software of each result are given in figures, blue regions represent the already activated (negative) areas and the red regions are the areas of cells which are not activated (positive) yet. The transition between two regions is called the wavefront.

5.2.1 Comparison of Conventional Regularization Methods

Figure 5.6 and 5.7 show the epicardial potential distrubution in Map3d, recovered inversely from the body surface potentials. The results are displayed at three different time instants. Four regularization methods, Tikhonov regularization, TSVD, LSQR and Bayesian MAP estimation, were employed and the results were compared with the measured epicardial potentials and with each other. Bayesian MAP estimation gives the best regularized epicardial potential disribution estimation due to the usage of training set properties, LSQR method gives the second best regularized epicardial potential distribution estimation. The LSQR method runs as an iterative algorithm. Therefore, it needs an optimum iteration number, which we obtained from the L-curve. Estimated epicardial potentials, that were obtained using Tikhonov regularization and TSVD, had similar potential maps. We used L-curve for choosing regularization parameters in Figure 5.8 and GCV for regularization parameters in Figure 5.10. The results are compared in three different time instants (t=39, 58, 67 seconds).

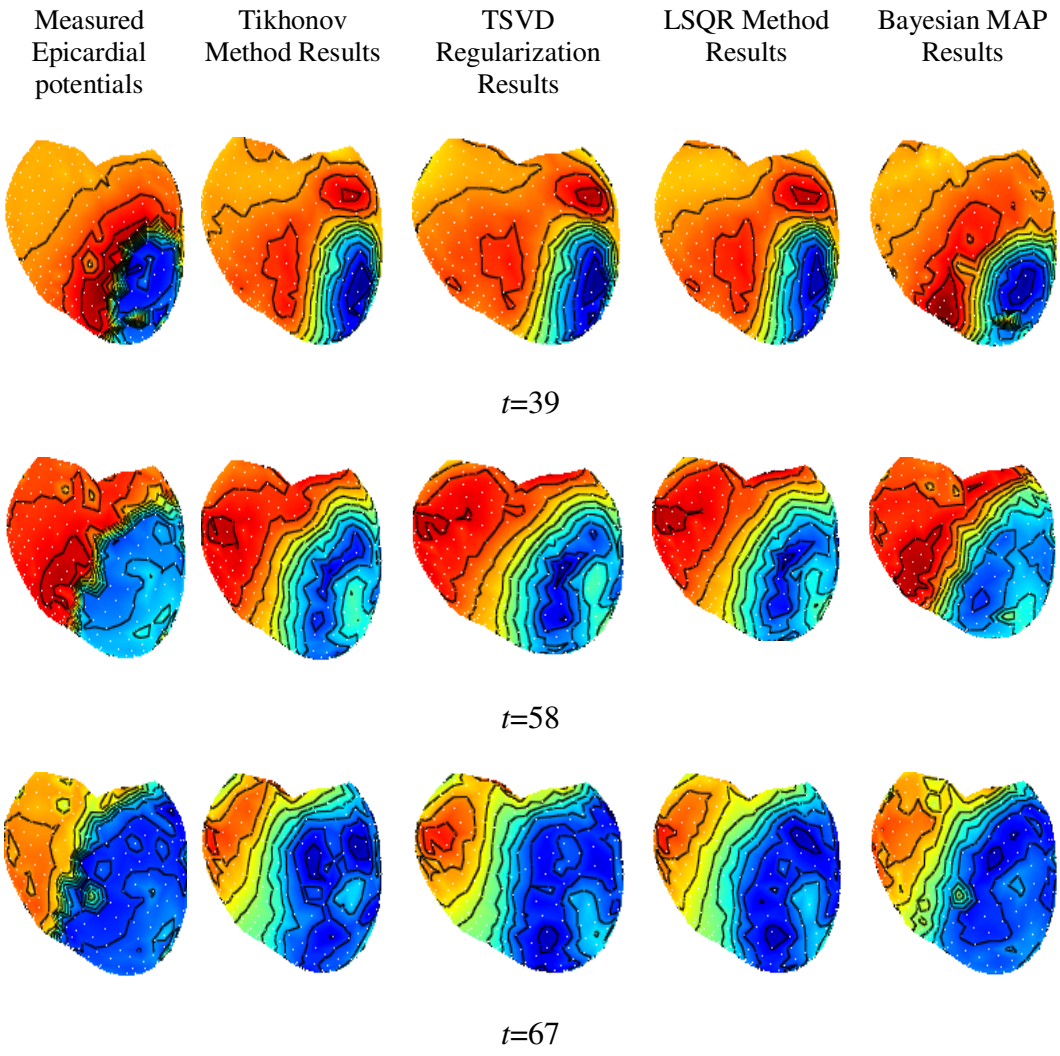

Figure 5.6 The comparison of the estimated epicardial potentials resulted for the four different conventional regularization methods at three different time instants, t=39, t=58, t=67 seconds (regularization parameters chosen from L-curve).

The perfomances of four regularization methods, which choose regularization parameters from L-curve, are given in Figure 5.6, 5.12, 5.13, 5.14 and Table 5.1. The performances of regularization methods, that chose their regularization parameters using the GCV, are given in Figure 5.7, 5.15, 5.16 and Table 5.2. It can be seen that Bayesian MAP estimation method always leads to a lower RE and higher CC compared with those of other methods.

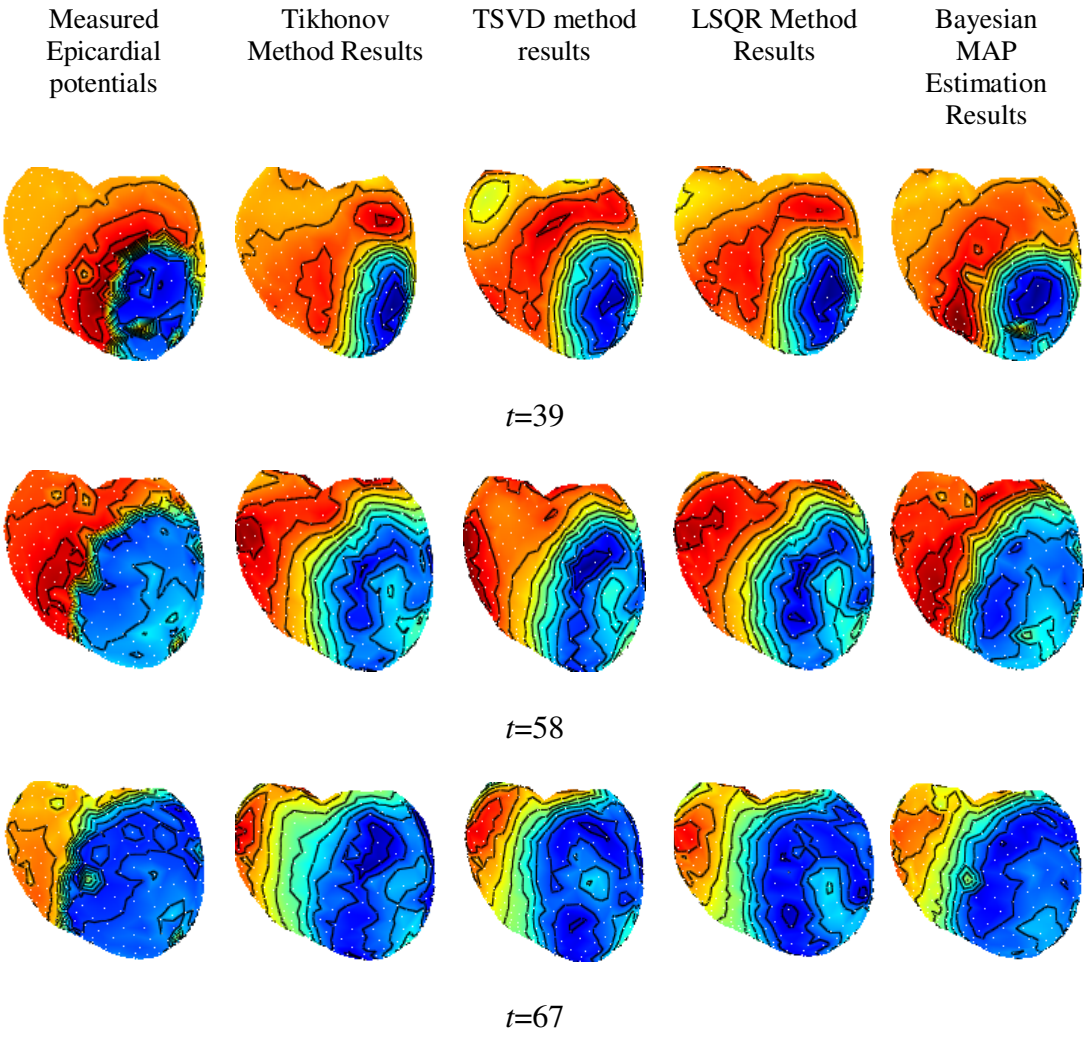

Figure 5.7 Comparing the known epicardial potentials with the estimated epicardial potentials resulted from four different regularization methods at three different time instants, t=39, t=58, t=67 seconds (regularization parameters chosen from GCV).

Table 5.1 RE and CC rate comparison of four regularization methods when using L-curve method

	Avg. RE ± std.	Avg. CC ± std.
Tikhonov	0.577±0.002	0.801±0.002
TSVD	0.601±0.002	0.788±0.004
LSQR	0.539±0.003	0.812±0.001
Bayesian MAP	0.523±0.003	0.841±0.002

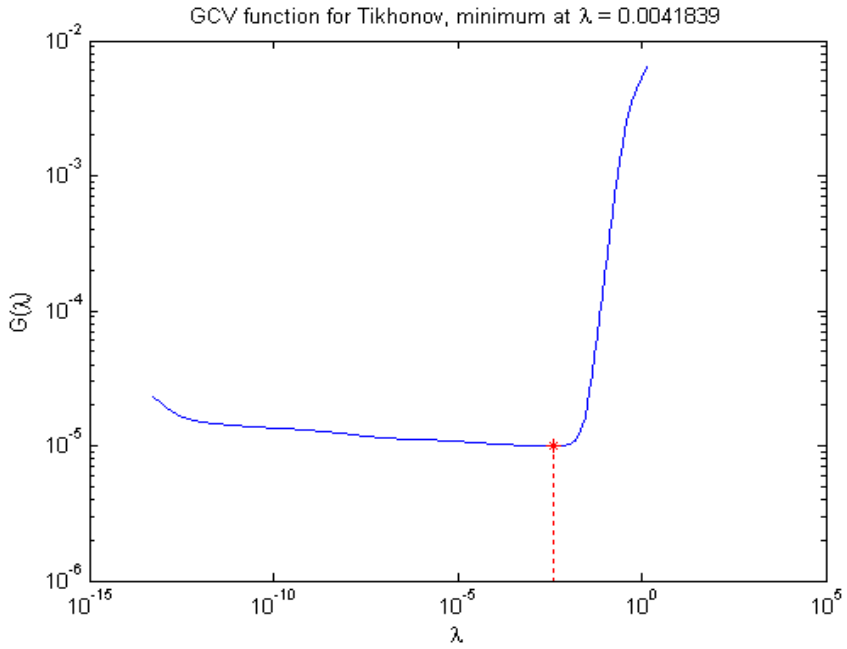

Figure 5.8 Regularization parameter chosen from GCV method for Tikhonov Regularization at time intance t=47

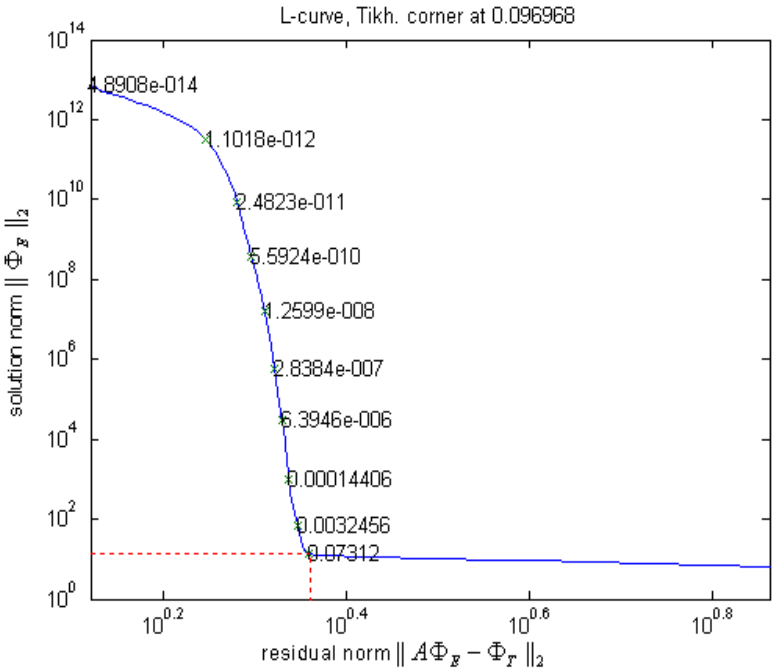

Figure 5.9 L-curve for choosing the regularization parameter for Tikhonov Regularization Method

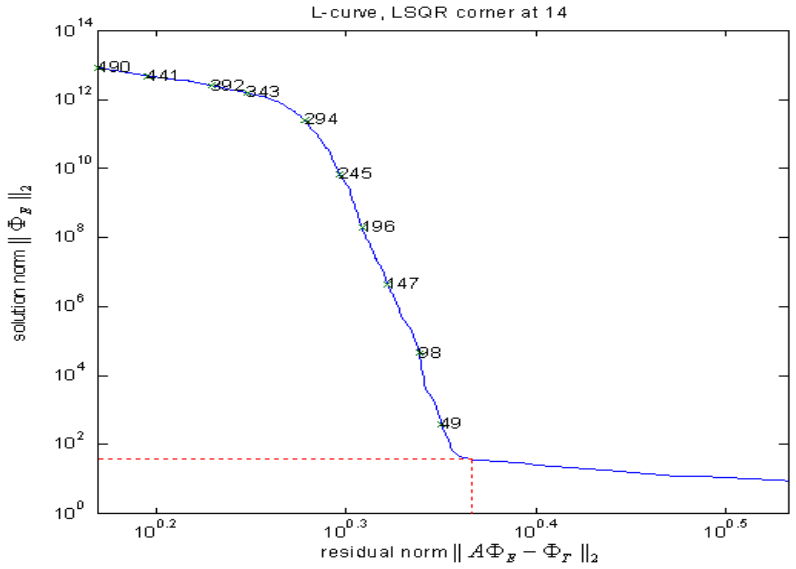

Figure 5.10 L-curve for choosing the iteration count for LSQR method (the optimum iteration is 14 which is the corner of the L-curve in this case).

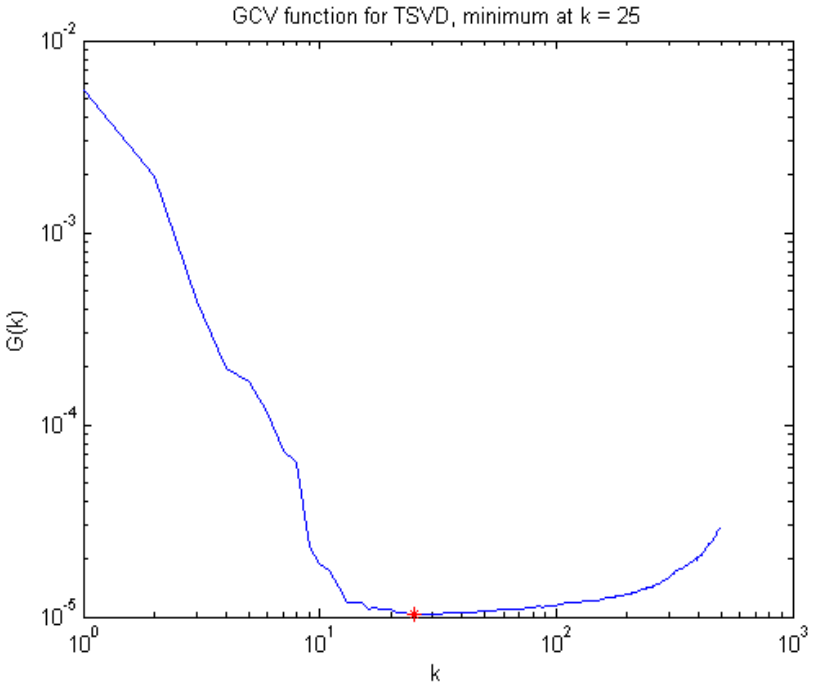

Figure 5.11 Regularization parameter chosen from GCV method for TSVD Regularization at time intance t=47 (the value of the chosen regularization parameter k =25 in this case).

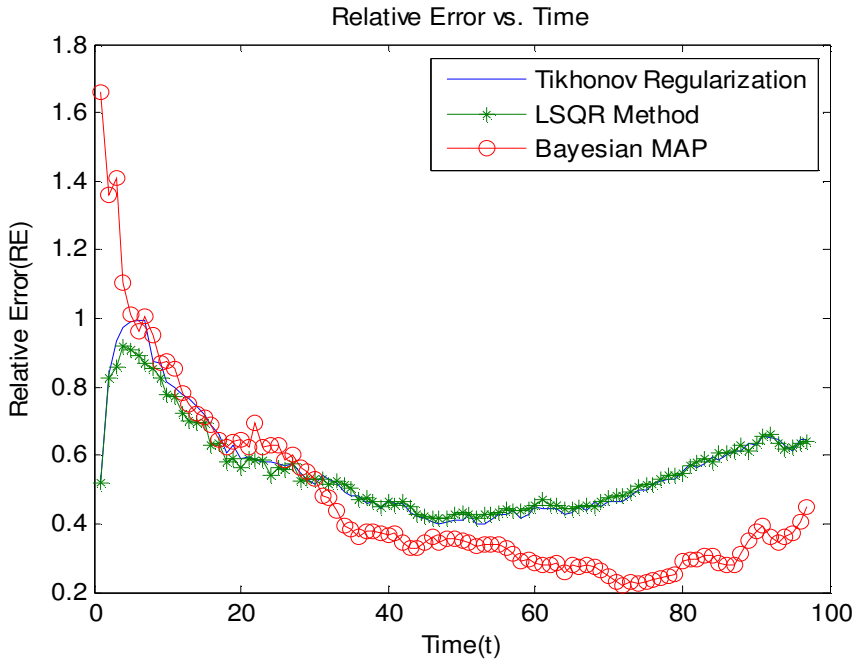

Figure 5.12 Comparison of the RE rate for three regularization methods (regularization parameter is chosen from L-curve method for Tikhonov Regularization and LSQR Method).

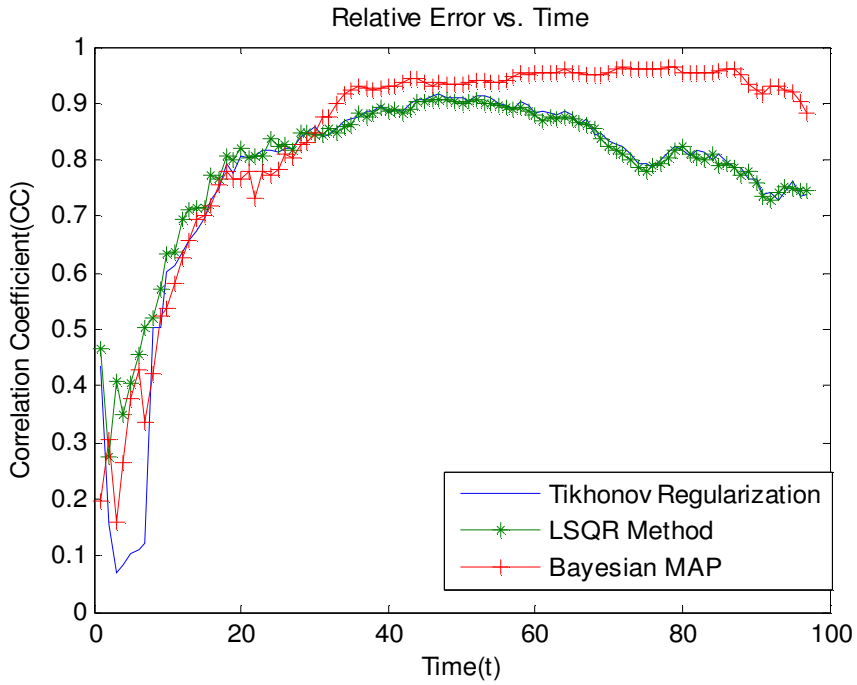

Figure 5.13 Comparison of the CC for three regularization methods, regularization parameter is chosen from L-curve method for Tikhonov Regularization and LSQR Method

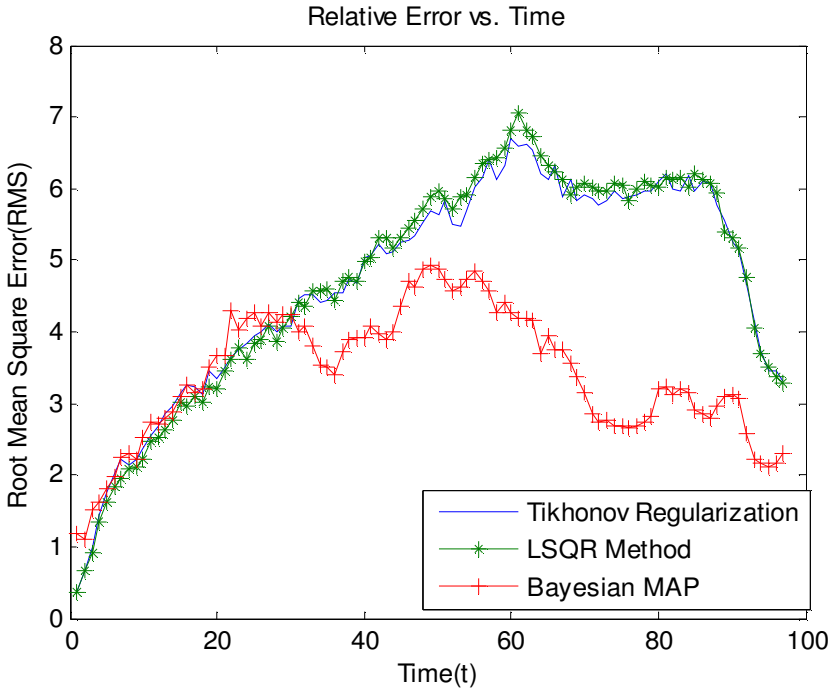

Figure 5.14 Comparison of the Root Mean Square(RMS) Error for three regularization methods, regularization parameter is chosen from L-curve method for Tikhonov Regularization and LSQR Method.

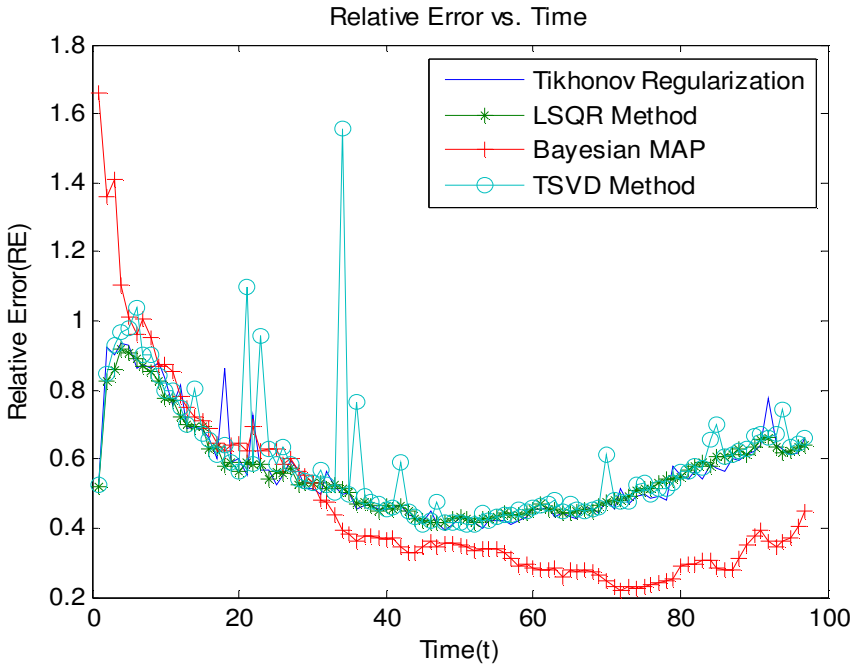

Figure 5.15 Comparison of the RE rate for four regularization methods, regularization parameter is chosen from GCV method for Tikhonov Regularization, TSVD and LSQR Method

The Tikhonov and TSVD Regularization solutions reflect the wavefront propagation pattern of the exact epicardial potential maps in general; however, they cannot follow the wavefront on the epicardium as well as the Bayesian solutions do. In Figure 5.12, 5.13 and 5.14 we see that Bayesian MAP Estimation method shows a better performance than Tikhonov Regularization and LSQR method with respective to smaller RE and higher CC. The LSQR method shows better performance than Tikhonov Regularization in early time instants; later it shows similar performance with Tikhonov Regularization. In Figure 5.15, we see that TSVD regularization method has bigger RE for some time instants because TSVD chose some bad regularization parameters using the GCV method. In order to see the RE of regularization methods clearly, we omited the RE results of TSVD then we plotted RE graph of three other regularization methods in Figure 5.16.

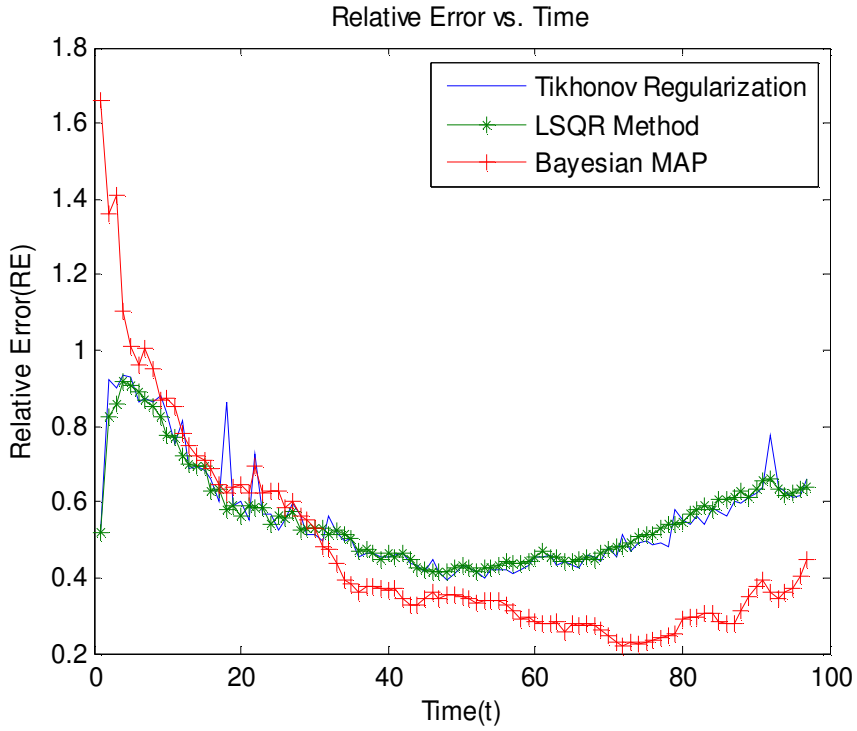

Figure 5.16 Comparison of the RE rate for three regularization methods, regularization parameter is chosen from GCV method for Tikhonov Regularization and LSQR Method.

Table 5.2 RE and CC rate comparison of four regularization methods when using GCV method

	Avg. RE ± std.	Avg. CC ± std.
Tikhonov	0.611±0.004	0.776±0.002
TSVD	0.748±0.004	0.701±0.002
LSQR	0.549±0.004	0.807±0.002
Bayesian MAP	0.524±0.003	0.839±0.002

Regularization methods behaved similar to the L-curve case when the regularization parameters which were chosen from GCV method in Figure 5.16 and in Table 5.2.

5.2.2 Comparison of Conventional Regularization Methods Combined with GA

In this section of this study, we give the simulation results of solution of inverse problem of ECG using regularization methods combined with GA. The simulation of the combination of conventional regularization methods and the GA is shown in Figure 5.17. And then we give the visual results of epicardial potentials using the tool Map3d and the comparison results of the obtained potentials and the initial epicardial potentials. The results of each regularization method are compared with exact epicardial potentials and with the results of regularization methods combined with GA. We compared them in two different cases. We used the minimization of equation 3.2 as the fitness function for GA in the first case. In the second case we had exact epicardial potentials and employ RE as the fitness function for the GA. The comparisons of all sections are based on these cases.

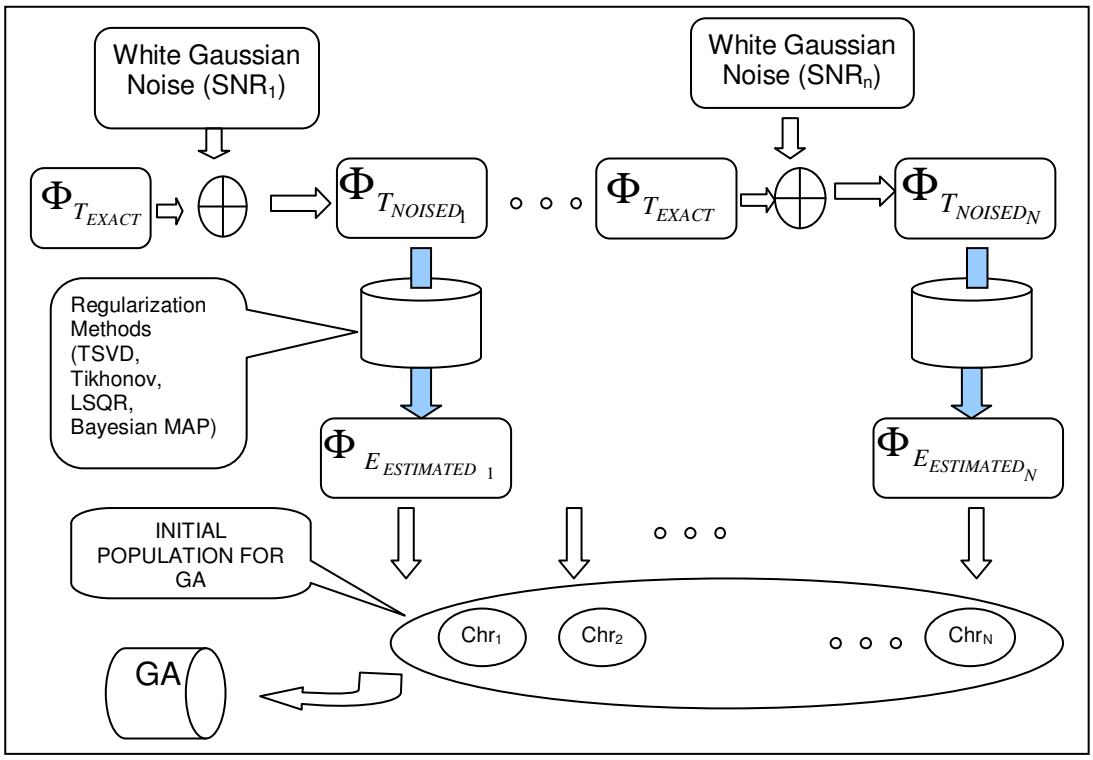

Figure 5.17 Combination of regularization methods and the GA

5.2.2.1 Tikhonov Regularization and GA

We employed Tikhonov Regularization for solving inverse ECG problem. We used the results of regularization as IP for the GA. There were ten noisy torso potentials which were obtained by adding 30 dB SNR with different seeds. After regularization we had ten estimated epicardial potentials. In GA case, we used two different fitness functions which were least squares minimization and the RE. The first fitness function is more realistic in clinical case, since the measured apicardial potentials must be known to calculate the RE. The results showed that combination of Tikhonov Regularization and the GA improves the regularization of ill-posed ECG problem. In Figure 5.18, we used the least squares minimization in (c) and the RE in (d) as fitness function. We used the known epicardial potentials for the second case.

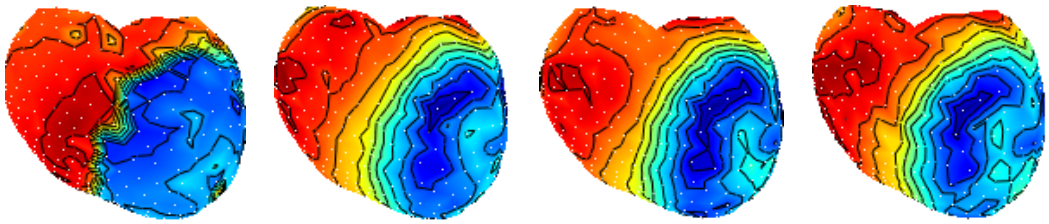

(a)	(b)	(c)	(d)
Measured Epicardial Potentials	Tikhonov Solution for epicardial potentials (30 dB SNR added exact torso potential)	1st GA result for population for Tikhonov Regularization Results (fitness function is the least squares minimization)	1st GA result for population for Tikhonov Regularization Results (fitness function is RE)

Figure 5.18 Comparing the known epicardial potentials with results of combination of Tikhonov Regularization and the GA for three different cases at time t=58

Table 5.3 RE and CC rate comparison of Tikhonov Regularization Results and combination of GA with Tikhonov Regularization Results.

	Avg. RE ± std.	Avg. CC ± std.
1st Tikhonov Regularization	0.560±0.001	0.788±0.001
2nd Tikhonov Regularization	0.559±0.001	0.787±0.001
1st GA Solution	0.551±0.001	0.801±0.001
2nd GA Solution	0.558±0.002	0.790±0.001

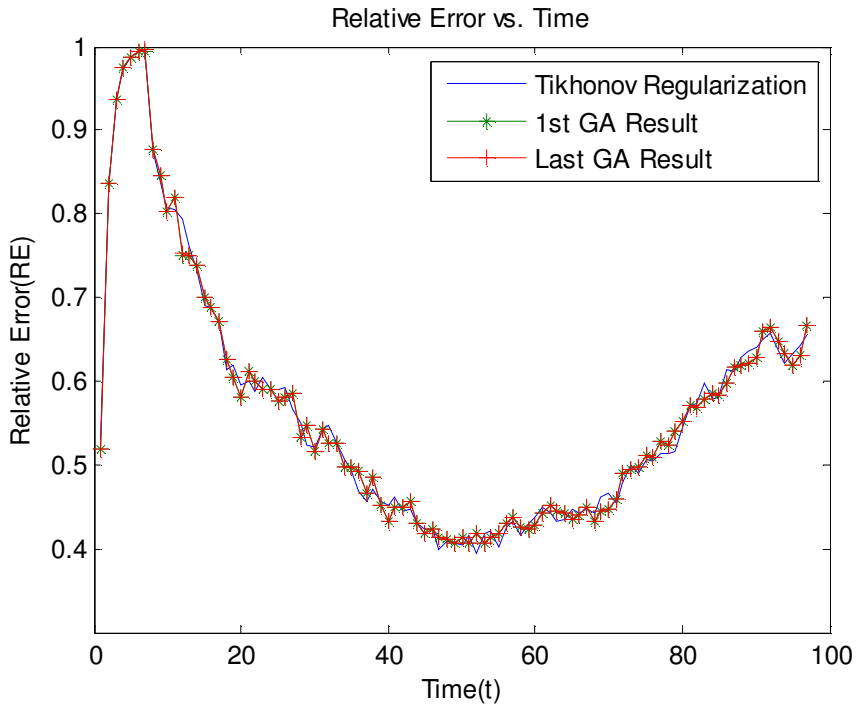

(a)

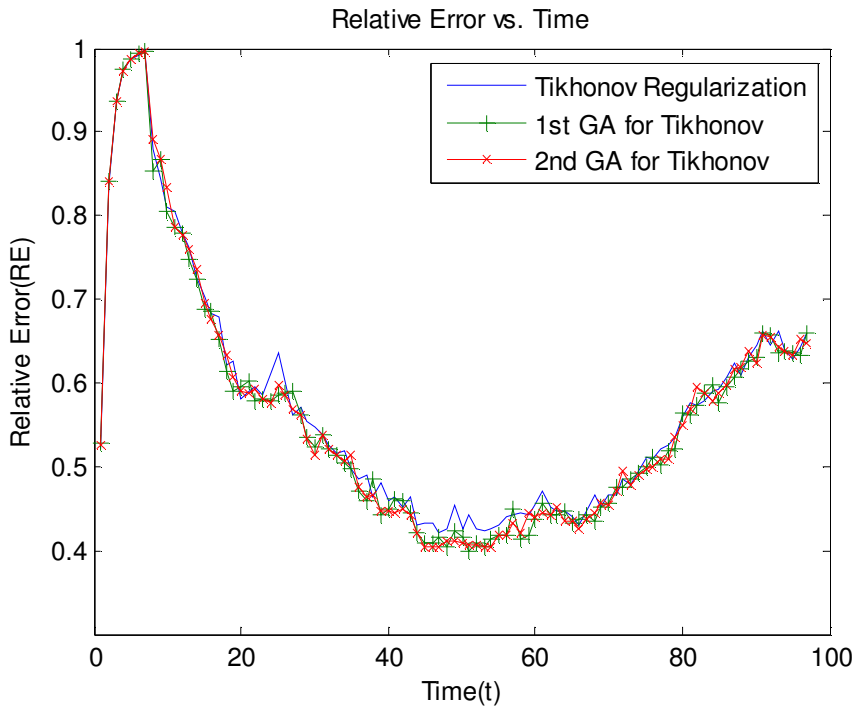

(b)

Figure 5.19 Mean RE plots of single Tikhonov Regularization results and the results of the combination of Tikhonov Regularization with the GA for two different fitness functions, (a) least squares minimization, (b) the RE with known epicardial potentials

The GA accomplished to improve the regularization and reduce the RE in Fig. 5.19. Also the generation number and the IP count are the critical parameters and effect the results of optimization. According to the results in Figure 5.19 and Table 5.3, GA could improve the regularization results of Tikhonov Regularization method. The GA's RE is smaller and CC is higher than single Tikhonov Regularization method's results.

5.2.2.2 TSVD Regularization and GA

Similar to Tikhonov Regularization same conditions were applied to TSVD Regularization. According to the results in Figure 5.20, we see the changes over the simulated epicardial potentials on the Map3d visual results. The second plot in Figure 5.21, the GA reduces the RE for TSVD regularization slightly. Also in Table 5.4, the GA combined TSVD method's RE is smaller and CC is higher than single TSVD Regularization method's results.

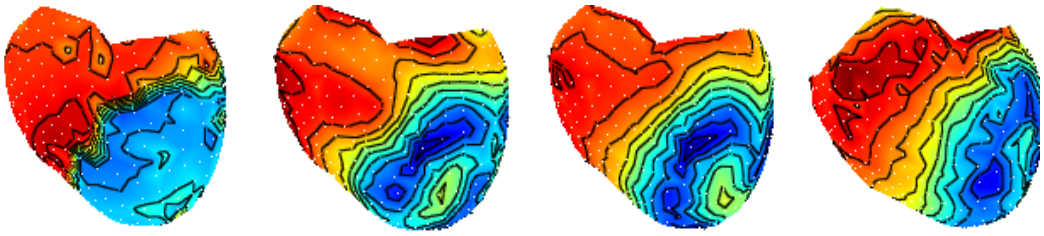

(a) Measured Epicardial Potentials

(b) TSVD Solution for epicardial potentials (30 dB SNR added exact torso potential)

(c) 1st GA result for population for TSVD Regularization Results (fitness function is the least squares minimization)

(d) 1st GA result for population for TSVD Regularization Results (fitness function is RE)

Figure 5.20 Comparing the known epicardial potentials with results of combination of TSVD Regularization and the GA for three different cases at time t=58 (regularization parameter from GCV)

Table 5.4 RE and CC rate comparison of TSVD Regularization and combination of GA with TSVD Regularization Results.

	Avg. RE ± std.	Avg. CC ± std.
1st TSVD Regularization	0.719±0.004	0.766±0.002
2nd TSVD Regularization	0.717±0.004	0.773±0.002
3rd TSVD Regularization	0.741±0.004	0.765±0.002
1st GA Solution	0.716±0.004	0.881±0.002
2nd GA Solution	0.719±0.002	0.869±0.001

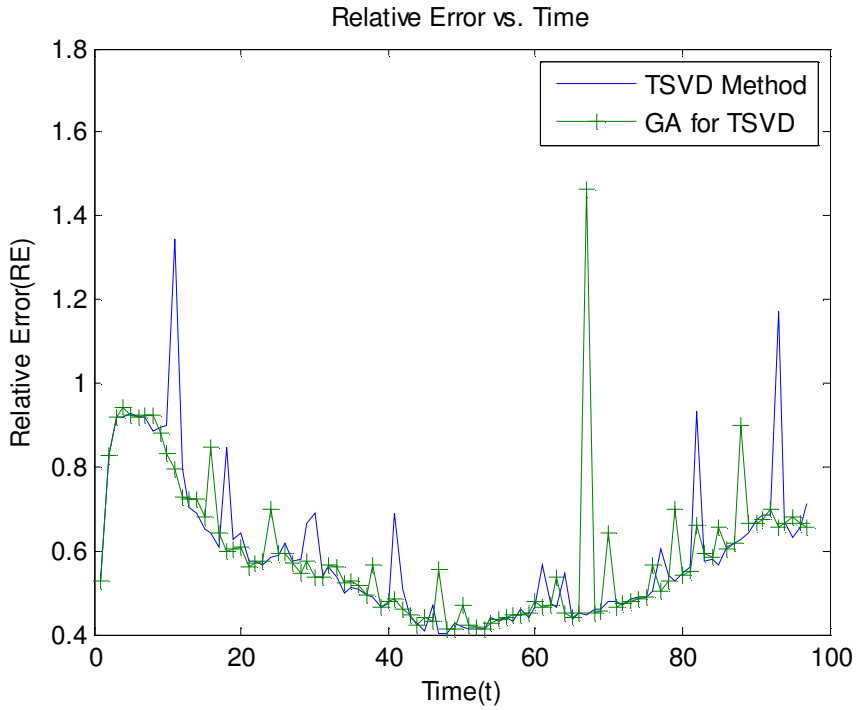

(a)

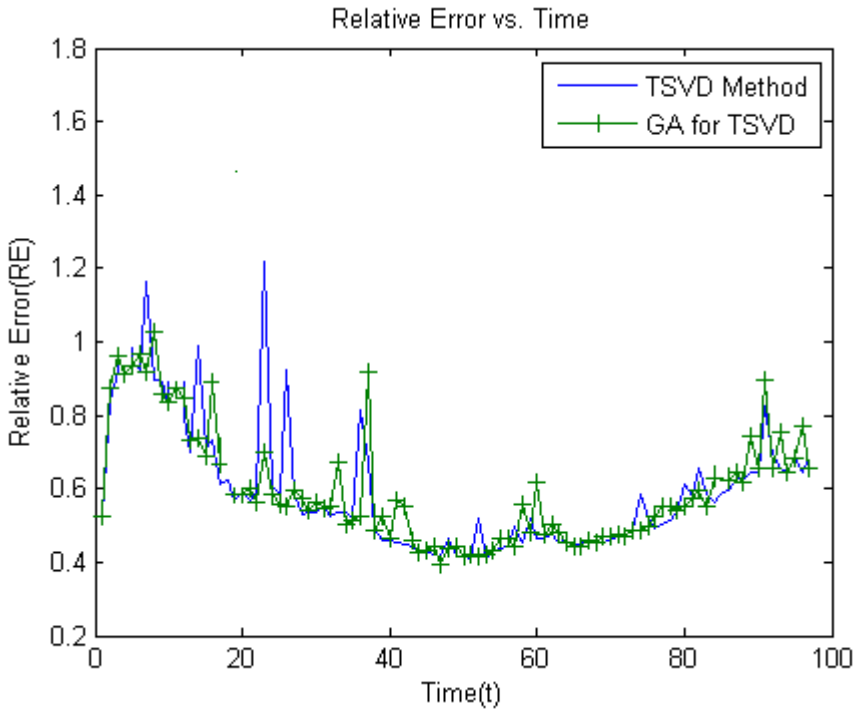

(b)

Figure 5.21 The RE rates of combination of TSVD Regularization with the GA, (a) fitness function is least squares minimization (3.2), (b) fitness function is RE using known epicardial potentials (regularization parameter from GCV)

5.2.2.3 Least Squares QR Method and GA

Figure 5.22 shows the Map3d visual results for LSQR regularization results and the GA combined regularization results for two different fitness functions used in GA. In the second case the visual results show that GA accomplishes to improve the reflection of the wavefront propagation pattern of the exact epicardial potential maps.

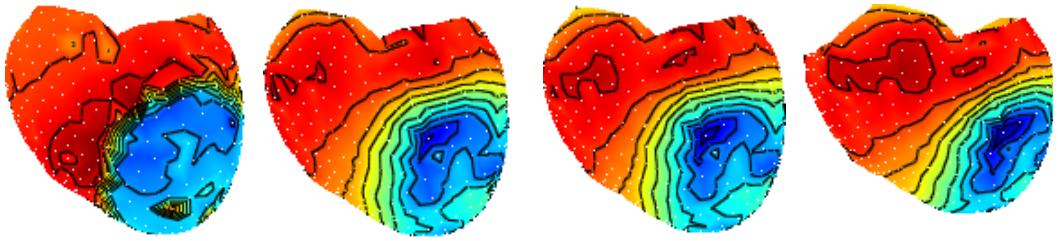

(a)	(b)	(c)	(d)
Measured Epicardial Potentials	LSQR Solution for epicardial potentials (30 dB SNR added exact torso potential)	1st GA result for population for LSQR Regularization Results (fitness function is the least squares minimization)	1st GA result for population for LSQR Regularization Results (fitness function is RE)

Figure 5.22 Comparing the known epicardial potentials with results of combination of LSQR Method with the GA for three different cases at time t=51

Table 5.5 RE and CC rate comparison of LSQR Regularization Results and combination of GA with LSQR Method Results

	Avg. RE ± std.	Avg. CC ± std.
1st LSQR Regularization	0.540±0.001	0.802±0.002
2nd LSQR Regularization	0.541±0.002	0.798±0.001
3rd LSQR Regularization	0.549±0.001	0.788±0.001
1st GA Solution	0.530±0.003	0.816±0.002
2nd GA Solution	0.537±0.002	0.807±0.001

The transfer matrix is an ill-posed matrix, so LSQR does not work efficiently very well in low SNR. However, the combination of GA and LSQR method produced relatively good solutions compared to using the single LSQR method. Since LSQR is an iterative method, we need an iteration number. If the optimum value for the iteration number (in Figure 5.8) is chosen, the smallest RE rate and the most accurate epicardial potential distribution can be obtained;

otherwise the solution converges to worse epicardial potential distributions. It was found that, a lower RE and higher CC were obtained by the combination method (see Figure 5.23 and Table 5.5).

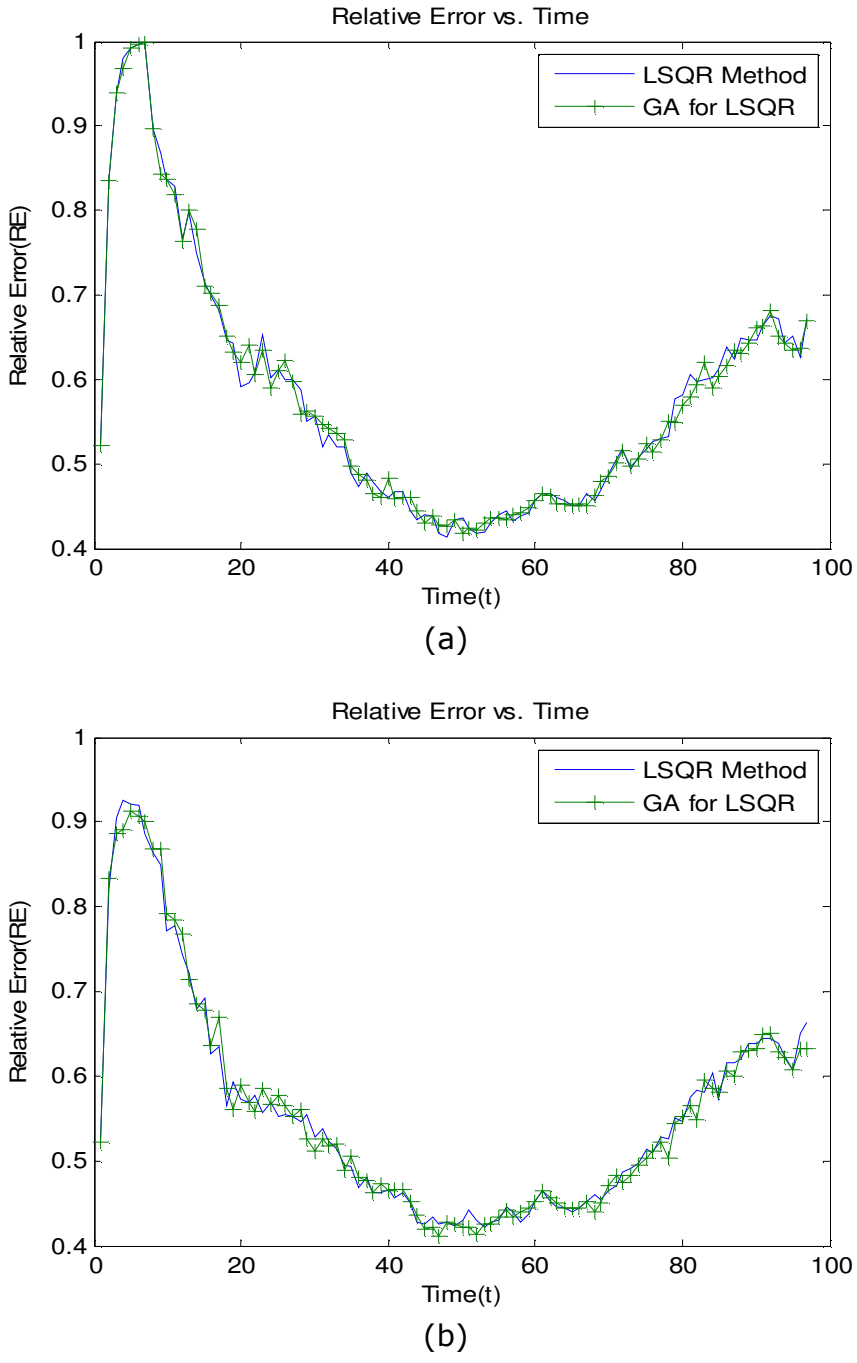

Figure 5.23 The RE rates of combination of LSQR Method with the GA, (a) fitness function is least squares minimization (3.2), (b) fitness function is RE using known epicardial potentials.

5.2.2.4 Bayesian MAP Estimation and GA

It can be easily seen in Figure 5.24 and 5.26 Bayesian MAP Estimation method has more resemblance to the original signal distrubutions than the regularization methods whose results are mentioned until this section. We compare the improvement of GA to the conventional regularization methods for optimizing the estimated epicardial potentials as axplained in detail in section 5.3.2.5. The covariance matrix was obtained from training set data for Bayesian MAP Estimation method. According to the RE rate in Figure 5.25 and Table 5.6, The GA did not improve the results of Bayesian MAP regularization as much as the results of other regularization methods.

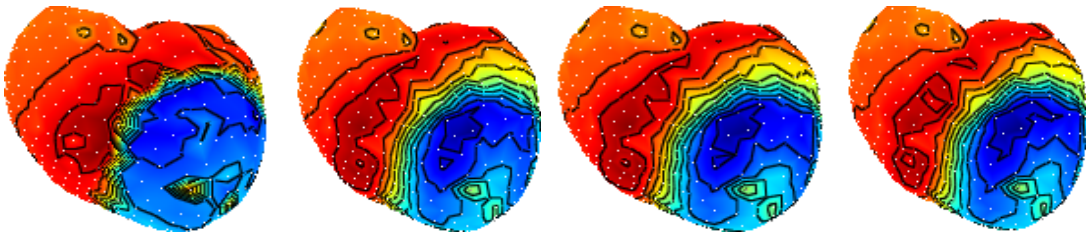

(a)	(b)	(c)	(d)
Measured Epicardial Potentials	Bayesian MAP Estimation Solution for epicardial potentials (30 dB SNR added exact torso potential)	1st GA result for population for Bayesian MAP Estimation Results (fitness function is the least squares minimization)	1st GA result for population for Bayesian MAP Estimation Results (fitness function is RE)

Figure 5.24 Comparing the known epicardial potentials with results of combination of Bayesian MAP Estimation with the GA for three different cases at time t=51

Table 5.6 RE and CC rate comparison of Bayesian MAP Estimation Results and GA combination of GA with Bayesian Method Results

	Avg. RE ± std.	Avg. CC ± std.
1st Bayesian MAP Est.	0.513±0.004	0.856±0.002
2nd Bayesian MAP Est.	0.517±0.004	0.841±0.002
3rd Bayesian MAP Est.	0.525±0.004	0.820±0.002
1st GA Solution	0.509±0.004	0.860±0.002
2nd GA Solution	0.517±0.002	0.840±0.001

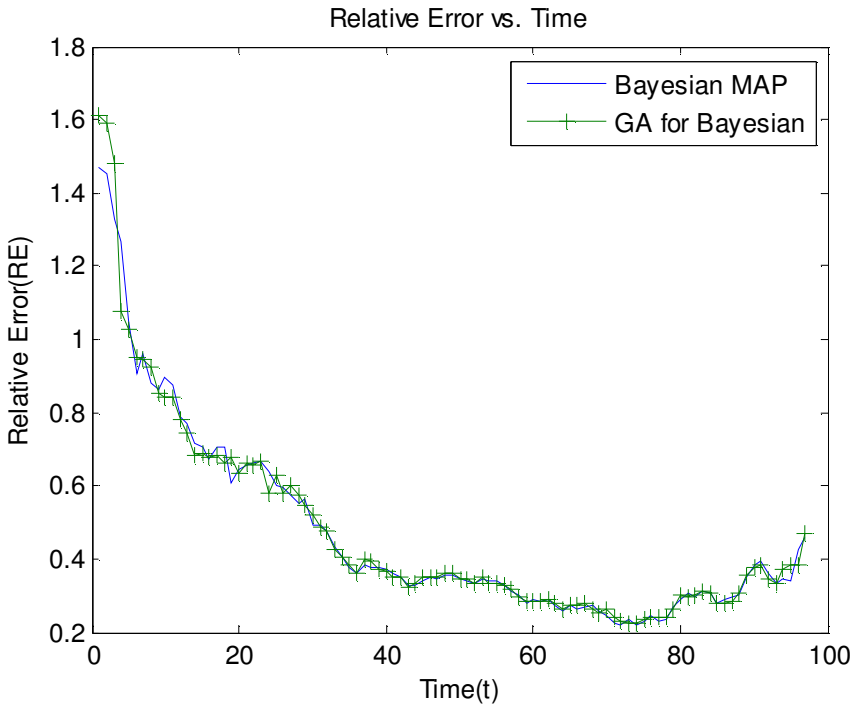

(a)

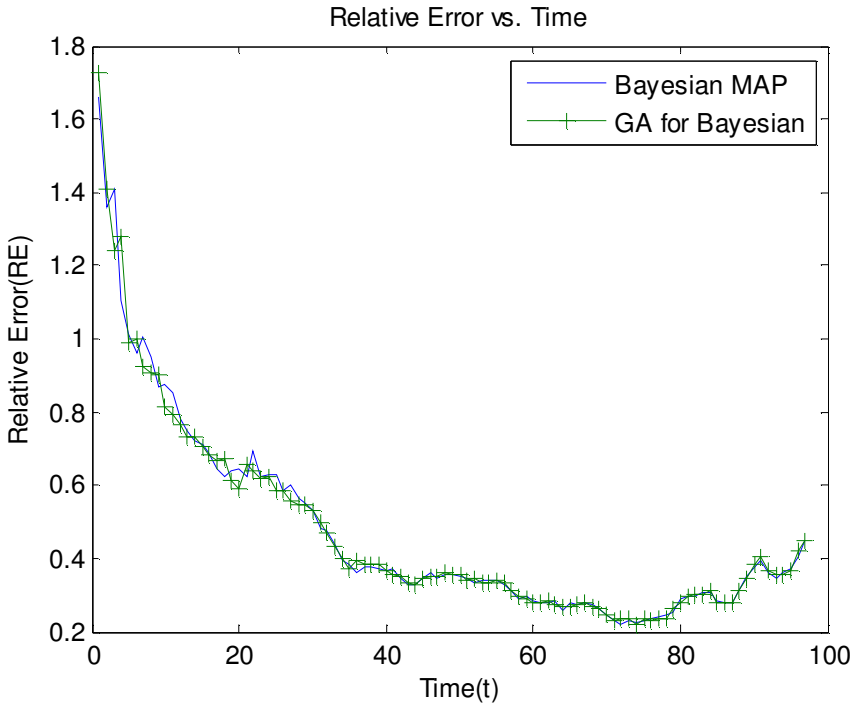

(b)

Figure 5.25 The RE rates of combination of Bayesian MAP Estimation with the GA, (a) fitness function is least squares minimization (3.2), (b) fitness function is RE using known epicardial potentials.

5.2.2.5 Conventional Regularization Methods and GA

In this section we compare the results of all regularization methods which were combined with GA. In Figure 5.26, Map3d visual results of estimated epicardial potentials are given for each regularization methods combined with GA at time instant t = 51. Figure 5.27 shows the RE graphs of the regularization methods combined with GA.

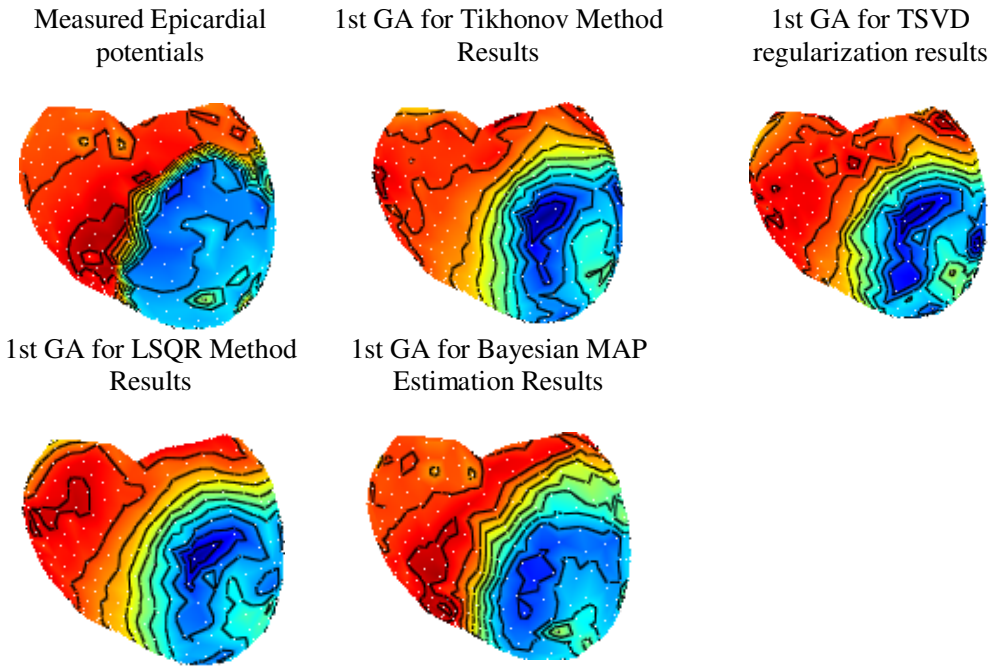

Figure 5.26 Comparing the known epicardial potentials with results of combination of four different regularization methods (Tikohonov Regularization, TSVD, LSQR and Bayesian MAP) with the GA at time t=51

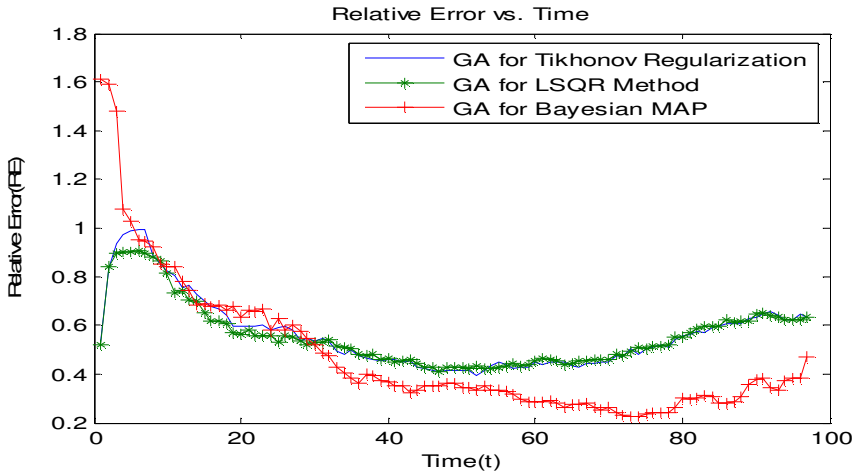

Figure 5.27 The RE rate for three regularization methods combined with the GA.

Bayesian MAP Estimation method's RE values are gradually decreasing and smaller than the other two methods. The LSQR method's RE values are smaller than Tikhonov Regularization method's RE values in early time instants, but later the values overlap.

5.2.2.6 Direct Application of the GA to Training Set

In this section, we had eight different epicardial potentials, called as training set, which we use as the IP for the GA. Our goal is to assess whether GA chooses some properties of training set potentials and produces reasonable inverse solutions. For this case, we bypassed the "regularization with conventional methods" part, and input eight different epicardial potential distributions (training set) directly into the GA process (Figure 5.28). We compared the results of this section with the results of combination of GA and Tikhonov Regularization. In Figure 5.29, the Map3d results are presented.

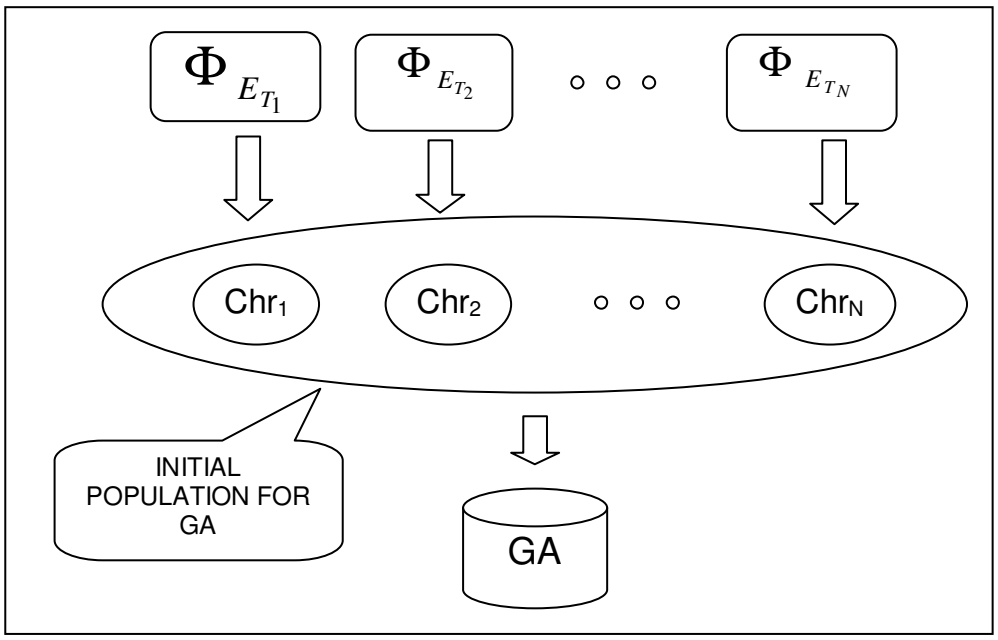

Figure 5.28 Applying GA to training set directly

According to the potential maps in these figures, application of GA to training set data, we got better estimated epicardial potentials than the potentials obtained from the combination of Tikhonov Regularization with GA. There is a decrease in RE for training set potentials compared to the RE for the estimated potentials obtained from the combination of Tikhonov Regularization with GA in Figure 5.30 and Table 5.7.

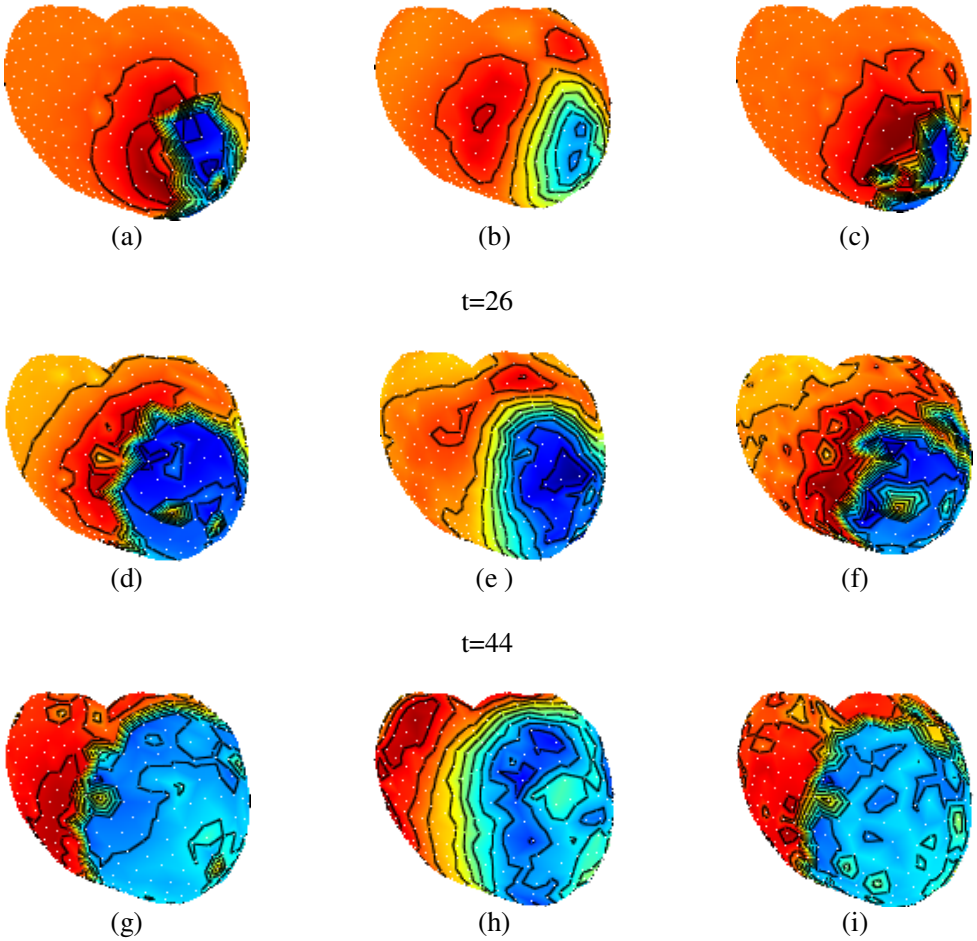

(a) (b) (c)

t=26

(d) (e) (f)

t=44

(g) (h) (i)

Measured Epicardial Potentials

Tikhonov Regularization Solution for epicardial potentials (30 dB SNR added exact torso potential) t=61

GA results for population of Training Set (fitness function is the least squares minimization)

Figure 5.29 Comparing the known epicardial potentials with results of Tikhonov Regularization and the GA applied training set epicardial potentials at time t=26, 44, 61

Table 5.7 RE and CC rate comparison of Tikhonov Regularization Result, 1st and 2nd GA Result for Training Set.

	Avg. RE ± std.	Avg. CC ± std.
Tikhonov Regularization	0.564±0.002	0.771±0.002
1st GA Solution	0.513±0.003	0.809±0.003
2nd GA Solution	0.529±0.003	0.797±0.002

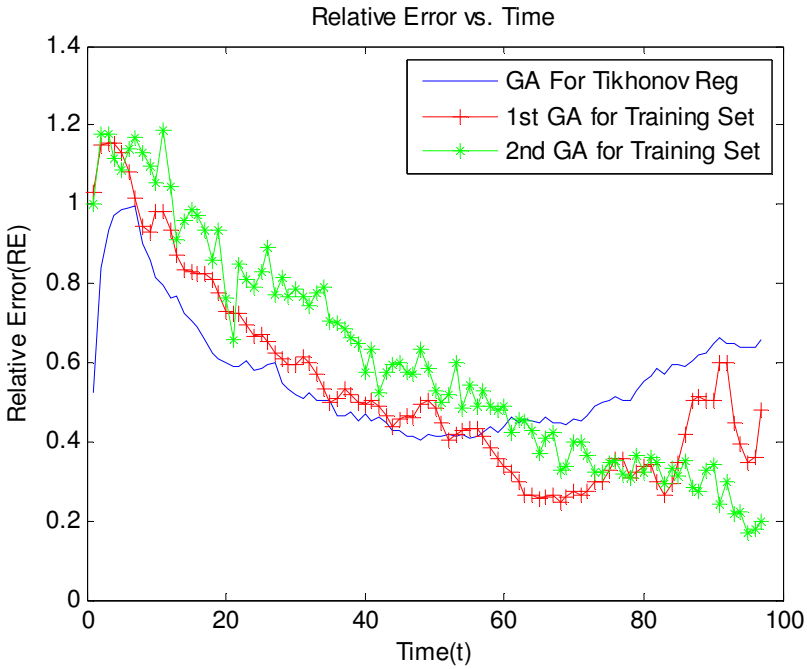

Figure 5.30 Comparison of the RE rate of Tikhonov Regularization Results, first and second GA results for Training Set

5.2.2.7 Using a Range of Regularization Parameters from L-curve

In this section we solved ill-posed inverse ECG using Tikhonov Regularization. This regularization method needs a regularization parameter to minimize squared norms of both the residual and the solution. The L-Curve is a generally accepted method to obtain the λ parameter. It is an L shaped curve, and the optimum λ corresponds to the corner of this curve. We used a number of regularization parameters around the optimum λ as shown in Figure 5.31. Here we plot the L-curve at t= 46th time and show the range of λ that is used in Tikhonov regularization. In this way, we obtained over-regularized and under-regularized solutions. These solutions were used for the IP chromosomes for the GA (Figure 5.32). According to the Map3d results of Tikhonov Regularization which uses a range of regularization parameters, GA produces an improved epicardial potentials compared to the optimum solution of regularization method in article (e) in Figure 5.33. We observed that the GA could choose the good features of over-regularized and under-regularized solutions and include them to the optimization phase. So we got an improved epicardial potential reconstruction. Figure 5.34 shows that the RE for GA is smaller than the RE of optimum regularization results. In Table 5.8 the mean RE and CC rate of the regularization methods are introuced.

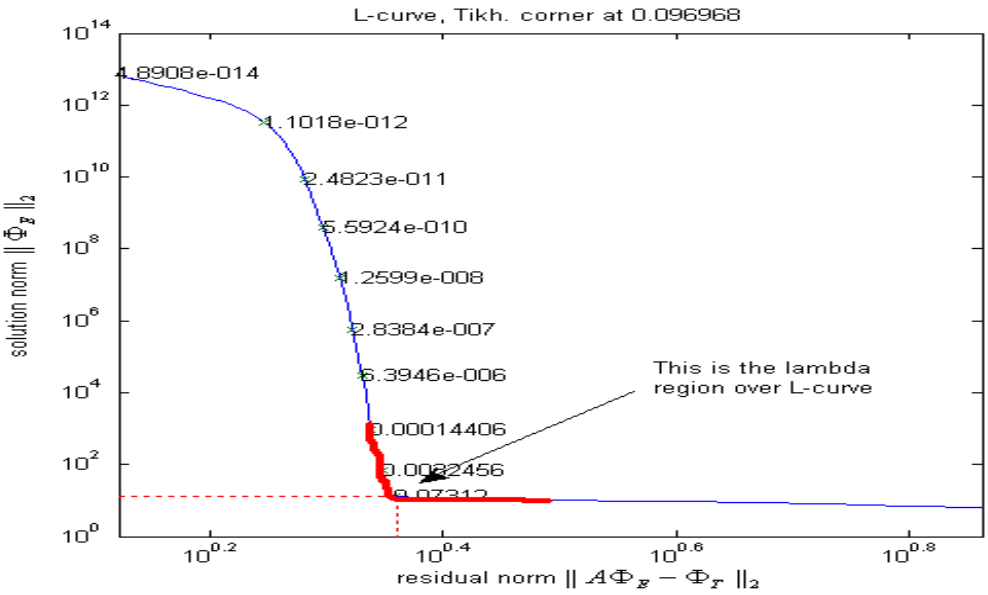

Figure 5.31 Choosing regularization parameters between under- and over-regularized region of L-curve

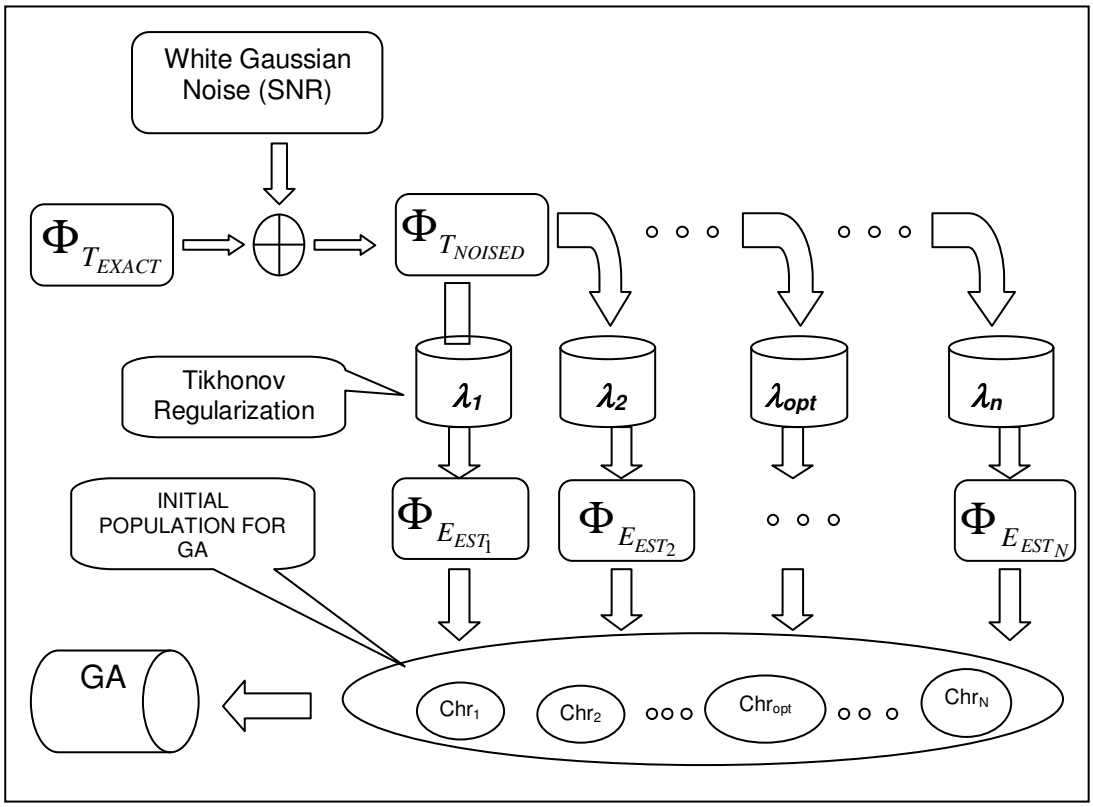

Figure 5.32 Application of GA to the results of Tikhonov Regularization by using a range of regularization parameters

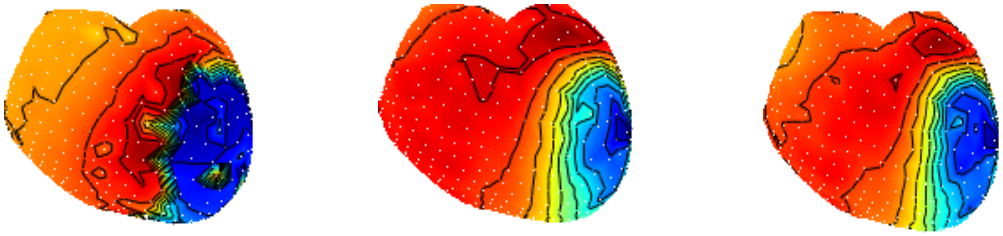

(a) Measured Epicardial Potentials

(b) Tikhonov solution with the over-regularized λ

(c) Tikhonov solution with the optimum λ

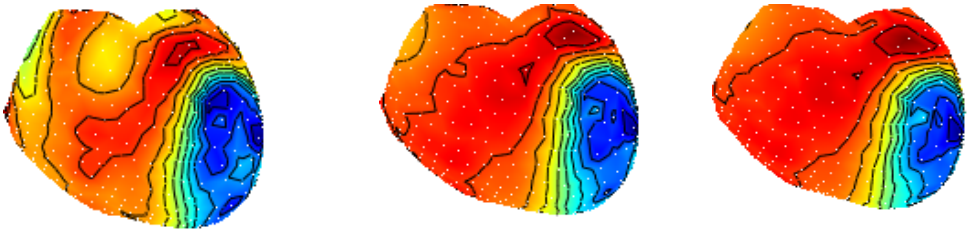

(d) Tikhonov solution with the under-regularized λ

(e) 1st GA Optimization Result for IP of λ ranges

(f) Last GA Optimization Result for IP of λ ranges

Figure 5.33 Comparing the known epicardial potentials with the over-regularized, under-regularized, the optimum Tikhonov Regularization results and the two GA results at time t=46

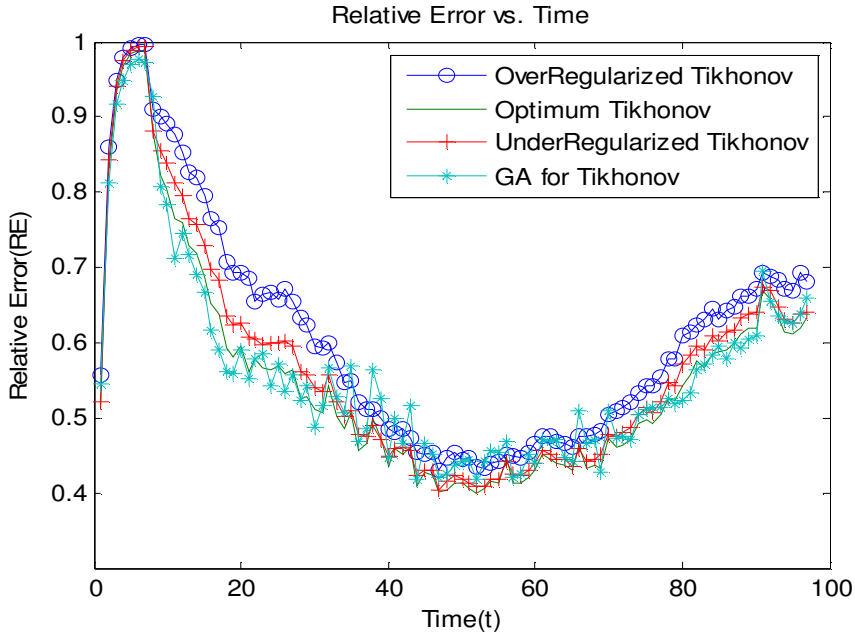

Figure 5.34 The RE rate of Tikhonov Regularization Results using regularization parameter optimum, under- and overregularized λ range, and the GA results which uses these regularization results as IP.

Table 5.8 RE and CC rate comparison of 1st GA Result and Tikhonov regularization method when using regularization parameters from a λ range from L-curve

	Avg. RE ± std.	Avg. CC ± std.
Tikhonov (Opt)	0.577±0.002	0.801±0.001
Tikhonov (Over)	0.713±0.003	0.557±0.003
Tikhonov(Under)	0.811±0.003	0.501±0.001
1st GA Result	0.516±0.002	0.851±0.003

5.2.2.8 Comparison of Bayesian MAP Estimation and the GA Results with the IP from a Training Set

In this section, we compare the results of Tikhonov Regularization, Bayesian MAP Estimation, combination of these methods with GA and the application of GA directly to the training set. Especially, the comparison focused on the Bayesian MAP Estimation results and the results of optimization when GA is applied to the training set directly. The performances of Tikhonov Regularization and Bayesian MAP Estimation are given in Figure 5.35.

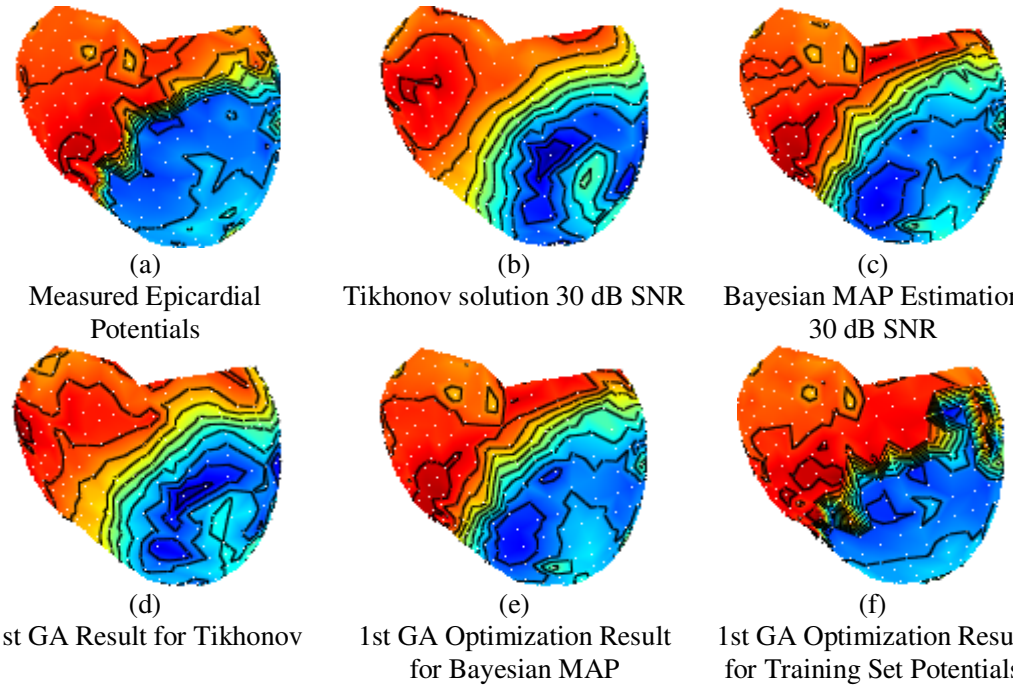

(a) Measured Epicardial Potentials

(b) Tikhonov solution 30 dB SNR

(c) Bayesian MAP Estimation 30 dB SNR

(d) 1st GA Result for Tikhonov

(e) 1st GA Optimization Result for Bayesian MAP

(f) 1st GA Optimization Result for Training Set Potentials

Figure 5.35 Comparing the improvement rate of regularization methods when GA applied to Bayesian MAP Results, Training Set and Tikhonov Regularization Results at time t=58

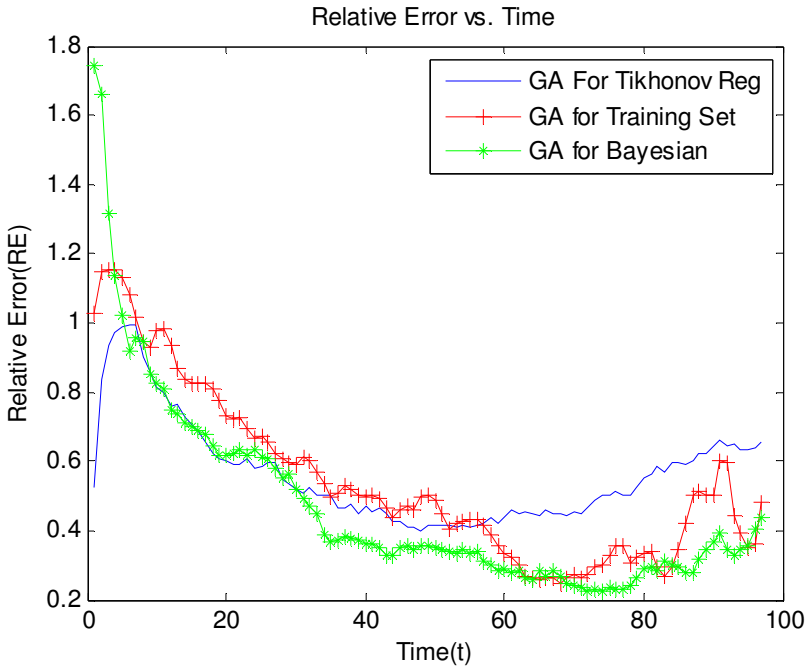

Figure 5.36 Comparison of RE rate for best GA results of Tikhonov Regularization, Bayesian MAP Estimation and Training Set

Also, the GA results for two regularization methods and training set are given in Figure 5.35. According to the visual potential map results, application of GA to training set directly produces better estimated epicardial (optimized) potentials than the other combined regularization methods. Bayesian MAP method also showed a good improvement to estimate epicardial potentials. Figure 5.36 shows the RE rate for estimated epicardial potentials. The RE is gradually decreasing in the GA with the training set as the IP, for the Bayesian MAP case the RE decreases to a minimum value and then there is a slight increase in RE rate and, the RE starts with low rate, it decreases then increases for the Tikhonov regularization solution. In Table 5.9 the mean RE and CC rate of the regularization methods are introuced.

Table 5.9 RE and CC rate comparison of single Tikhonov Regularization, single Bayesian MAP Results, best results of combination of GA with Tikhonov Regularization, Bayesian MAP Estimation and Training Set

	Avg. RE ± std.	Avg. CC ± std.
Tikhonov Regularization	0.564±0.002	0.770±0.002
Bayesian MAP Estimation	0.472±0.003	0.842±0.002
1st GA Solution for Tikhonov Reg.	0.552±0.002	0.792±0.002
1st GA Solution for Bayesian MAP	0.456±0.003	0.865±0.002
1st GA Solution for Training Set	0.513±0.003	0.808±0.002

5.3 Discussions

Regularization is the key step in solving inverse problems. The most well-known regularization methods, such as the Tikhonov regularization method and the TSVD method reduce noise in different ways. The Tikhonov regularization method requires constraints such as restricted energy of the computed epicardial potentials. The TSVD method truncates the small singular values to reduce the noise influence. In both regulzarization methods, we use singular value decomposition of transfer matrix which has an ill-conditioned property. If this matrix is large, then the decomposition of this matrix is an expensive operation. The LSQR method is an iterative regularization method which is based on bidiagonalization procedure. The LSQR method does not need the SVD of the transfer matrix to solve inverse problems. It produces estimated epicardial potentials at the end of each iteration. This method requires an optimum iteration number to stop processing. If we do not stop iteration after this iteration number, the method may converge to a worse solution with a high RE. Tikhonov regularization method and TSVD also require an optimum regularization parameter and an optimum truncation number, respectively, for solving inverse problems. We use the well-known methods, the L-curve and the GCV, to obtain optimum regularization parameters, We found that the L-curve method usually produces more stable solutions. We use another method to solve inverse ECG problem which is called Bayesian MAP Estimation. When the epicardial potentials are assumed to be Gaussian distributed, it needs a covariance matrix and a mean vector to solve the problem. In this study, we assumed that the mean vector is the zero vector, and we obtained the covariance matrix from epicardial potentials from a training set.. Finally, we combined the regularization methods with the GA. For each regularization method we employed the GA process. If we run GA sufficient number of times, we get more improved epicardial potentials. Also the GA parameters affect the optimization rate. These parameters are obtained by trial and error methodology. There are many studies to determine the GA parameters in literature. Also the application of GA directly to the training set and the combination of GA with Tikhonov method which uses regularization parameters from a range on L-cuve may be a good scheme for solving the inverse ECG problem.

CHAPTER 6

CONCLUSIONS

The inverse ECG problem is ill-posed, and regularization has to be applied in order to obtain stable and reliable solutions. There are several studies in literature that develop regularization methods to overcome this obstacle. A detailed study has been undertaken to evaluate the performance of some of the conventional regularization methods for solving inverse ECG problem. We used four different methods to estimate the epcardial potential, such as Tikhonov Regularization, TSVD, LSQR and Bayesian MAP Estimation methods. We solved the problem by each method using column sequential method to ignore temporal constraints. In this study, we combined the regularization methods with the GA. We compared the simulation results of the single regularization methods and the GA combined regularization methods. According to the results, the GA contributed to the regularization method to improve the regularization. In addition to the above studies, two new approaches were proposed by us:

- We solved inverse ECG running Tikhonov regularization which used a range of regularization parameters which were chosen around the optimum regularization parameter from L-curve. We obtained under-regularized, optimum and over-regularized epicardial potential estimations. We used these estimated epicardial potentials to construct the IP for the GA. We got improved epicardial potentials which had smaller RE and higher CC.
- We applied GA to traning sets data directly to see whether GA produces better epicardial potentials when compared to the results of conventional regularization methods. In this case, we had the exact epicardial potentials, we added 30 dB white Gaussian noise the exact torso potential which we calculated by multiplication of transfer matrix and exact epicardial potentials. We used this perturbed torso potential in fitness function to minimize the norm of residual. We obtained improved epicardial potentials with respect to the results of other regularization methods.

Finally, we compared the estimated epicardial potentials using the RE, CC, RMS error plots and the visual tool Map3d. According to the results, Bayesian MAP solutions have better error performances and results than those of the Tikhonov, TSVD and LSQR solutions, since we have

used a covariance matrix that was obtained from training set data for Bayesian MAP Estimation method.

As a summary, the conventional regularization methods solve the inverse ECG problem. They use different solution methods which were given along the thesis. Each regularization methods has some advantages or disadvantages over the other regularization methods. Combination of regularization methods with GA for solving inverse ECG provides us with better estimated epicardial potentials.

6.1 Future Work

We will apply the GA to the mixed results of different regularization methods. By using this methodology, we can see whether the GA takes better sides of each regularization methods results or not. We will apply the CRESO method to the regularization methods which requires regularization parameter. Then the GA will be applied the results of regularization methods which uses CRESO method. We will compare the results of these new applications with the old results that we obtained in this thesis. Finally, we will improve the user friendly properties of the GUI.

REFERENCES

[1] World Health Report, 2007, The World Health Organization (WHO), http://www.who.int/cardiovascular_diseases/en/.

[2] Waller, A.D., *A demonstration on man electromotive changes accompanying the heart's beat*, J. Pysiol. 8: 229–34, 1887.

[3] Malmivuo, J., and Plonsey, R., *Bioelectromagnetism - principles and applications of bioelectric and biomagnetic fields*, Oxford University Press, New York, 1995.

[4] Bianco, C., *How Your Heart Works*, http://www.howstuffworks.com/heart.htm.

[5] Lee, D., Kulick, D., and Marks, J., *Heart Attack (Myocardial Infarction) by MedicineNet.com*, Retrieved November 28, 2006.

[6] Burton, F. L., and Cobbe, S. M., *Dispersion of ventricular repolarization and refractory period*, Cardiovasc. Res., vol. 50, pp. 10–23, 2001.

[7] Netter, F.H., *Physiology and Functional Neuroanatomy. Nervous System I*, CIBA-GEIGY Ltd., Basle, 1989.

[8] Huiskamp, G., and Van Oosterom, A., *Forward electrocardiography based on measured data*, Engineering in Medicine and Biology Society, 1989

[9] Gulrajani, R. M., *The forward and inverse problems of electrocardiography*, IEEE Engineering in Medicine and Biology, 84/101, September/October, 1998.

[10] Gulrajani, R. M., Roberge, F. A., and Savard, P., *The inverse problem of electrocardiography*, in Macfarlane, P. W. and Lawrie, T. D. Veitch (Eds): Comprehensive Electrocardiology, 237–288, Pergamon Press, Oxford, England, 1989.

[11] Greensite, F., and Huiskamp, G., *An improved method for estimating epicardial potentials from the body surface*, IEEE Trans. Biomed. Eng. 45, 98–104, 1998.

[12] Skipa, O., *Linear inverse problem of electrocardiography: epicardial potentials and transmembrane voltages*, Helmesverlag Karlsruhe, 2004.

[13] Rudy, Y., and Plonsey, R., *The eccentric spheres model as the basis for a study of the role of geometry and inhomogeneities in electrocardiography*, IEEE Trans Biomed Eng, vol. 26, no. 7, pp. 392–399, 1979.

[14] Barr, R., and Spach, M., *Inverse calculation of QRS-T epicardial potentials from body surface potential distributions for normal and ectopic beats in the intact dog*, Circ. Res., vol. 42, pp. 661–675, 1978.

[15] Oostendorp, T. F., Van Oosterom, A., and Huiskamp, G., *Interpolation on a Triangulated 3D Surface*, Journal of Computational Physics, Academic Press, Num 80, pp.331–343, 1989.

[16] Greensite, F., Huiskamp, G., and Van Oosterom, A., *New quantitative and qualitative approaches to the inverse problem of electrocardiology: their theoretical relationship and experimental consistency*, Med Phys., May-Jun;17(3):369–79, 1990.

[17] Bourbaki, N., *Topological Vector Spaces*, Chapters 1-5. Elements of Mathematics. Springer. ISBN 3-540-13627-4, 1987.

[18] Colton, D., Engl, H. W., Louis, A. K., McLaughlin, J. R., and Rundell, W., *Surveys on solution methods for inverse problems*, Springer Verlag Austria, 2000.

[19] Golub, G. H., and Loan, C. F. V., *Matrix Computations*, The Johns Hopkins University Press, 1996.

[20] Tikhonov, A. N., and Arsenin, V. Y., *Solutions of ill-posed problem*, Winston&Sons, New York, 1977.

[21] Orck, A.B., Grimme, E., and Van Dooren, P., *An implicit bidiagonalization algorithm for ill-posed systems*, BIT, 34:510–534, 1994.

[22] Larsen, R.M., *Lanczos bidiagonalization with partial reorthogonalization*, PhD thesis, Dept. Computer Science, University of Aarhus, DK-8000 Aarhus C, Denmark, Oct. 1998.

[23] Golub, G.H., and Van Loan, C.F., *Matrix Computations (3rd ed.)*, Johns Hopkins, ISBN 978-0-8018-5414-9, 1996.

[24] Foster, M., *An application of the Wiener-Kolmogorov smoothing theory to matrix inversion*, J. Soc. Ind. Appl. Math., vol. 9/3, pp. 387–392, 1961.

[25] Jackson, D.D., *The use of a priori data to resolve non-uniqueness in linear inversion*, Geophys. J.R. astr. Soc., vol. 57, pp.137–157, 1979.

[26] Franklin, J.N., *Well-posed stochastic extension of ill-posed problems*, J.Math. Anal. Appl., vol. 31, pp. 682–716, 1970.

[27] Serinagaoglu, Y., Brooks, D. H., and MacLeod, R. S., *Bayesian solutions and performance analysis in bioelectric inverse problems*, IEEE Trans. Biomed. Eng., vol. 52, no. 6, pp. 1009–1020, 2005.

[28] Serinagaoglu, Y., Brooks, D. H., and MacLeod, R. S., *Improved performance of bayesian solutions for inverse electrocardiography using multiple information sources*, IEEE Trans. Biomed. Eng., vol. 53, no. 10, pp. 2024–2034, 2006.

[29] Hansen, P. C., *Rank-deficient and discrete ill-posed problems: Numerical aspects of linear inversion*, SIAM, 1998.

[30] Anderson, E., Bai, Z., Bischof, C., Blackford, S., Demmel, J., Dongarra, J., Croz, J. D., Greenbaum, A., Hammarling, S., McKenney, A., and Sorensen, *D., LAPACK Users' Guide*, SIAM, 3 ed., 1999.

[31] Hansen, P. C., and O'Leary, D. P., *The use of L-curve in the regularization of discrete ill-posed problems*, SIAM J. Sci. Comput., vol. 14, no. 6, pp. 1487–1503, 1993.

[32] Gulrajani, R., Roberge, R., and Savard, P., *The inverse problem of electrocardiography, in Comprehensive Electrocardiology (P. Macfarlane and T.T.V.Lawrie, eds.)*, vol. 1, pp. 237–288, Pergamon Press, 1989.

[33] Darwin, C., *The origin of species by means of natural selection*, London & Toronto, J.M. Dent & sons, 1928.

[34] Kuilekov, M., Ziolkowski, M., and Brauer, H., *Application of Genetic Algorithm to an Inverse Field Problem in Magnetic Fluid Dynamics*, Serbian Journal of EE, Vol.1, No.1, 1-13, 2003.

[35] Goldberg, D.E., *Genetic Algorithms in Search, Optimization and Machine Learning*, Addison Wesley, Readin, MA, 1989.

[36] Jiang, M., Xia, L., Shou, G., and Tang, M., *Combination of the LSQR method and a genetic algorithm for solving the electrocardiography inverse problem*, Phys. Med. Biol. 52 (2007) 1277-1294.

[37] Jiang, M., Xia, L., and Shou, G., *The Use of Genetic Algorithms for Solving Inverse Problem of Electrocardiography*, EMBS Annual International Conference, 2006.

[38] MacLeod, R.S., Lux, R.L., and Taccardi, B., *A possible mechanism for electrocardiographically silent changes in cardiac repolarization*, J. Electrocardiol., Vol. 30, Suppl.: 114-121, 1997.

[39] Macleod, R.S., and Johnson, C.R., *Map3d: Interactive scientific visualization for bioengineering data*, Datasets, Proc. Eng. Med. Biol. Soc. 15th Ann. Int. Conf., vol. 44, pp. 196–208, 1997, http://software.sci.utah.edu.

[40] Johnston, P. R., and Gulrajani, R. M., *A new method for regularization parameter determination in the inverse problem of electrocardiography*, IEEE Trans. Biomed. Eng. 44(1), 19–39, 1997.

[41] Johnston, P. R., and Gulrajani, R. M., *Selecting the corner of the L-curve approach to Tikhonov regularisation*, IEEE Trans. Biomed. Eng. 47(2), 1293–1296, 2000.

[42] SippensGroenewegen, A., Spekhorst, H., Van Hemel, N. M., Kingma, J. H., Hauer, R. N.W., De Bakker, J.M. T., Grimbergen, C. A., Janse, M. J., and Dunning, A. J., *Localization of the site of origin of postinfarction ventricular tachycardia by endocardial pace mapping. Body surface mapping compared with the 12-lead electrocardiogram*, Circulation, 88 (5), 2290– 2306, 1993.

[43] Lu, W., and Xia, L., *Computer simulation of epicardial potentials using a heart-torso model with realistic geometry*, IEEE Trans. Biomed. Eng. 43 211–7, 1996.

[44] Xia, L., Huo, M., Wei, Q., Liu, F., and Crozier, S., *Analysis of cardiac ventricular wall motion based on a threedimensional electromechanical biventricular model*, Phys. Med. Biol. 50 1901–17, 2005.

[45] Chu, C.H., and Delp, E.J., *Nonlinear methods in electrocardiogram signal processing, Center for Advanced Computer Studies, University of Southwestern Louisiana*, Lafayette, J. Electrocardiol, 23 Suppl:192-7, 1990.

[46] Brooks, D., and MacLeod, R., *Electrical imaging of the heart*, IEEE Sign. Proc. Mag., vol. 14, pp. 24–42, 1997.

[47] Hodgkin, A. L., and Huxley, A. F., *A quantitative description of membrane current and its application to conduction and excitation in nerve*, J. Physiol., vol. 177, pp. 500–544, 1952.

APPENDIX A

A GRAPHICAL USER INTERFACE FOR SOLVING INVERSE PROBLEM OF ECG

The application is a Windows Application based on Microsoft.Net Framework. It uses matlab regularization routines [29] which are compiled as dll (dynamic link library) and refereced in application. The regularization part is solved in matlab side.

It works in the following way;

1. User enters some number of SNR values to the interface,
2. Choosing the genetic algorithm parameters
    a. Population size
    b. Fitness scaling
    c. Selection
        - Rolulette
        - Tournament*
        - Custom
    d. Crossover
        - Scattered*
        - Custom
    e. Maximum generation number
    f. Mutation Type
        - Gaussian
        - Uniform*
        - Custom
    g. Mutation Rate
    h. Fitness Function

* Default parameters for the program

    i. Crossover Rate
3. Choosing regularization methods
    a. Tikhonov Regularization
    b. TSVD
    c. LSQR
    d. Bayesian MAP Estimation
    e. TGSVD
4. Choosing the regularization parameters finding method
    a. L-curve
    b. GCV
    c. CRESO
5. Start Solution (During solution phase user can choose to see the L-curve graph, GCV graph, RE graph or plot biggest error). Problem solution based on column sequential method,
6. After reconstructing estimating epicardial potentials from each noised torso potentials by using regularization methods, GA process starts, the noised eliminated solutions are the IP for the GA,
7. GA process stops if:
    a. the improvement rate of generations less than a specified rate,
    b. the iteration number is greater than the generation count,
    c. the RE is less than the specified rate for each result (we assume that we know the exact epicardial potentials) and not reach the maximum number of iteration (generation count).
8. Results, wich are shown through the interface, are:
    a. RE rate for each chromosomes,
    b. CC rate for each chromosomes,
    c. Residual norm for each chromosomes with the noiseless initial epicardial potentials.
9. After solutions are obtained, user can visualize the epicardial geometry and data using Map3d tool from its interface. In the left part of the interface user can choose the results and the noiseless data to compare the difference, in this case, user can choose noiseless data, one result from regularization methods and one result from GA to decide how efficient the GA to improve regularization methods and to lessen noise.

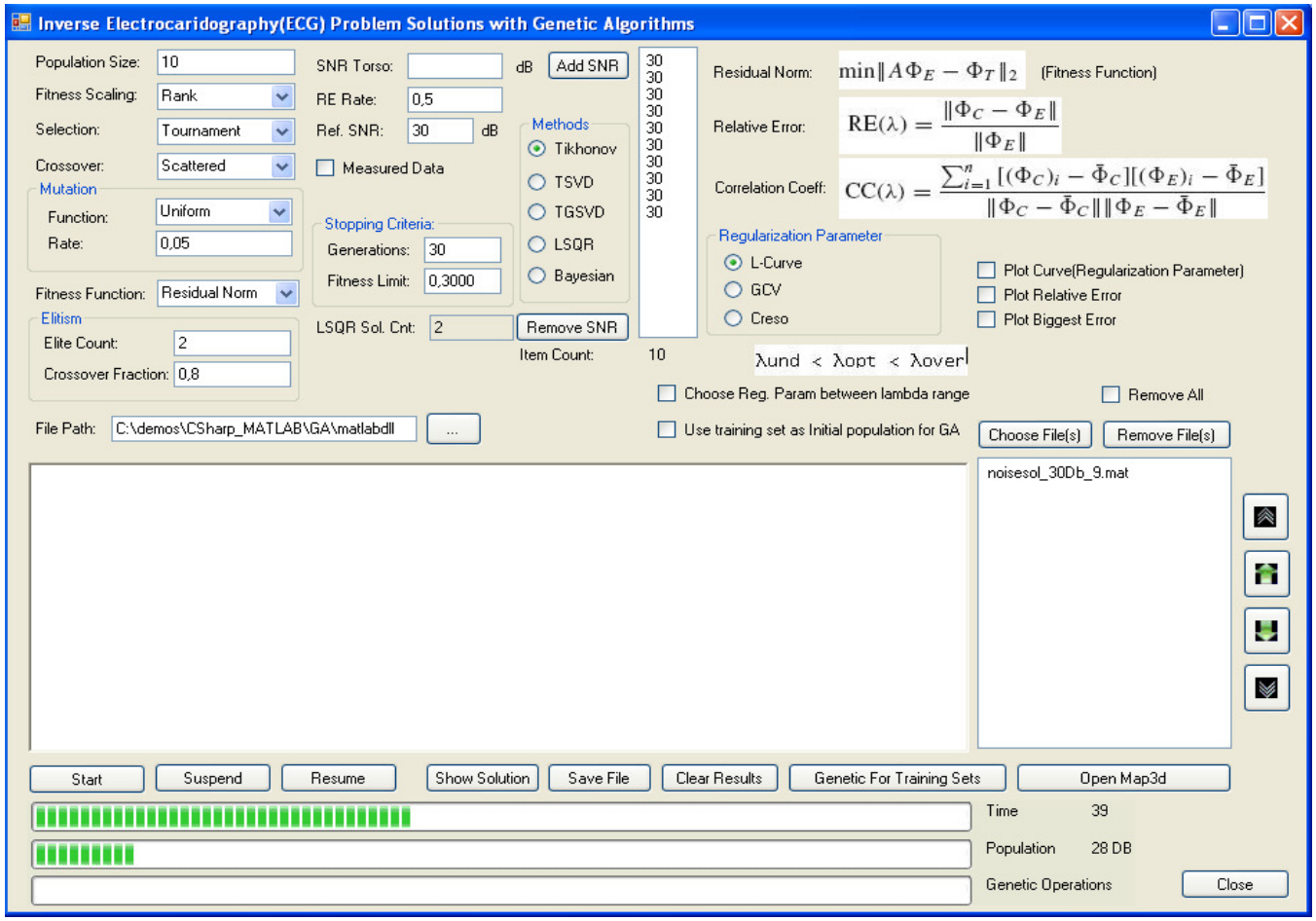

Figure A.1 A graphical user interface to solve the inverse ECG problem using regularization methods and their combination with the genetic algorithm

APPENDIX B

CLASSIFICATION OF ELECTROPHYSIOLOGICAL CARDIAC MODELS

Basically the classification of electrophysiological cardiac models can be subdivided into two main categories: mono- and bidomain modeling as well as rule-based modeling. The former considers the heart to consist of two subspaces, extra-and intracellular, being separated with the cell membrane. The membrane contains ion channels which allow ions of certain types to pass through it. The conductivity of ion channels changes according to the potential difference between the subspaces (transmembrane voltage (TMV)). Thus a large amount of differential equations must be solved in order to simulate electrophysiology of myocardium. This task requires huge computational efforts, strong parallelization and large volumes of memory, but leads to very precise results.

Rule-based modeling, on the other hand, considers the excitation of small patches of ventricular tissue based on certain rules ignoring the nature of this excitation. These patches possess relatively large size (typically 1×1×1mm3), thus the memory consumption is moderate. The action potential curve, refractory times and excitation conduction velocity are not computed in the course of modeling, but selected from a database according to certain criteria. Thus the calculation time decreases dramatically (several minutes against several days for the bidomain models on a single workstation), which allows for the use of cardiac modeling in everyday clinical practice. Due to the relative simplicity of this approach, several cardiac models based on this principle have been developed [35, 38, 40, 43, 44].

1. General Scheme of Myocardial Cell Models

The first quantitative model of an excitable cell was proposed by Hodgkin and Huxley in [41]. They considered the cell membrane as an electrical circuit containing a capacity and three resistances plugged in parallel (Figure B.1). The resistances were defined for the currents of sodium and potassium ions flowing through the corresponding ion channels, as well as for a small ”leakage current” made up by chloride and other ions. The resistance for the latter current was considered to be constant, whereas the former two resistances were changing with the transmembrane voltage.

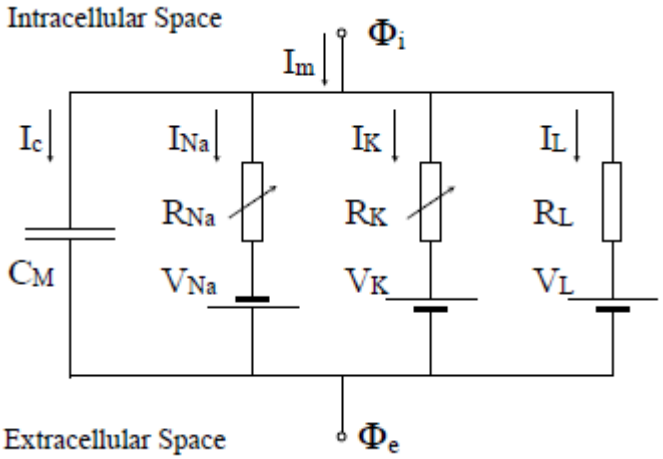

Figure B.1. The Hodgkin-Huxley representation of the cell membrane. Here Imrepresents the transmembrane current, Φi and Φe are the intra- and extracellular potentials, with transmembrane voltage: Vm= Φi– Φe. IN a, IK and IL represent the sodium, potassium and leakage currents, RNa, RK and RL– corresponding resistances and VNa, VKand VL- corresponding Nernst potentials. CM is the capacitance of the cell membrane.

The total current through the cell membrane can be written as follows:

$$I = C_M \cdot \frac{dV_m}{dt} + I_{Na} + I_K + I_L, \tag{B.1}$$

where I is the overall current through the cell membrane, CM is the capacitance of the cell membrane, Vm is the transmembrane voltage (TMV), INa, IK and IL represent the sodium, potassium and leakage currents, correspondingly. The ionic currents through the membrane can be computed by:

$$I_{Na} = g_{Na} \cdot (V_m - V_{Na}), \tag{B.2}$$

$$I_K = g_K \cdot (V_m - V_K), \tag{B.3}$$

$$I_L = g_L \cdot (V_m - V_L), \tag{B.4}$$

where VN a, VKand VL are the Nernst potentials for sodium, potassium and leakage ions [3], which are defined by the difference of concentration of the ion types inside and outside the cell, and gNa, gK and gL are the corresponding conductivities. The latter are defined by the fraction of opened channels for each type of ions. They change according to first order differential equations. The rate constants of these differential equations depend on the TMV. This model is able to correctly describe the excitation of an axon.

2. Cellular Automaton

A cellular automaton based model of the heart used in the present work belongs to the rule-based heart models. This model does not consider the interaction between the intra- and extracellular spaces in order to simulate the excitation propagation. Instead, a set of rules is defined for this propagation. The action potential curves are not computed ”on-the-fly”, but rather chosen from a predefined library. Thus a high performance and low memory consumption are assured, although the method is by far not as flexible as the bidomain methods.

A cellular automaton is applied to simulate the excitation propagation throughout the heart. If a voxel is depolarized, under certain conditions the neighboring voxels get excited as well. A voxel is considered as neighboring to a given one, if they have a common face or if they are connected with a segment of the excitation conduction system.
The excitation is conducted between the voxels if the following conditions are met:

1. Both voxels are excitable.
2. Both voxels belong to the same tissue or to tissues, between which the excitation conduction is allowed. For example, the direct conduction of excitation from atria to ventricles and vice versa is forbidden. On the contrary, the excitation propagation between Purkinje fibers and ventricular myocardium is allowed.
3. The voxel receiving the excitation should not be already excited. In other words, the myocardial tissue within the voxel should not be in refractory state.

For a normal heart beat, the excitation starts in the AV-node with a given frequency defining the heart rate. Afterwards the excitation propagates through the excitation con-duction system and reaches the ventricular myocardium. An extrasystolic beat can be modeled by introduction of a spontaneous excitation somewhere in the myocardium. Then the excitation is conducted through the myocardium until it reaches the excitation conduction system. Afterwards the excitation is spread over the endocardium by the conduction system. So the “all-or-nothing” principle is fulfilled independently from the origin of excitation.

3. Body Surface Potential Mapping (BSPM)

The technique known as Body Surface Potential Mapping (BSPM) involves sampling potentials at a greater number of sites on the torso surface (in the range of 32–256 electrodes). The wave forms of ECG signals recorded at the body surface depend not only on the heart’s electrical activity, but also on the positions of the electrode pairs used. When multiple lead positions are used, each lead provides a different aspect of the heart’s electrical activity. The display of a set of instantaneous potential data on a map representing the body surface is called a Body Surface Map

(BSM). The increasing experimental and clinical use of BSPM has shown that such maps can be related to certain regional electrical processes in the heart.

A body surface map is a low resolution projection of cardiac electrical events filtered by the torso cavity. With this greater amount of information, it is necessary to display this information in a useful manner and interpret the information in accordance with known electro-physiological principles to provide an accurate assessment of the cardiac state. These data can be interpreted directly in the form of potential maps with pattern matching techniques as is now accepted in Japan for daily clinical diagnosis [45]. However, the ability to determine details of regional electrical activity in the heart from visual inspection of the BSPM is limited. There have been some directions made towards identifying sites of reentry based on visual examination of QRS integral maps [46]. A better prospect would involve processing the large quantity of data through some form of mathematical modelling, to unravel the filtering effects of the torso and recover the electrical information at the heart level (i.e., solving the inverse problem of electrocardiography). Accurate solutions of the inverse problem from body surface maps will have great benefit for improving diagnosis and hence decisions about the treatment of patients. For the successful noninvasive computational calculation of cardiac sources, high quality body surface potential data must be obtained as the input for an inverse solution. The practical acquisition of high quality data is a non-trivial matter. However, this is becoming easier with the development of disposable electrode strips and portable multichannel recording systems.

APPENDIX C

GENETIC ALGORITHM PARAMETERS

1. Selection Types

- **Roulette Selection**

Each individual in population is assigned a probability value of being selected which is the proportionate of the fitness of them. Two chromosomes are then chosen randomly based on these probability values and produce new generation.

- **Tournament Selection**

It is one of the selection methods in GAs which runs a tournament among the individuals of the population chosen randomly from the current generation and selects the best fitting individual for crossover easily adjusted by changing the size of the tournament. The worst fitting individuals have small probability to be selected, If the size of the tournament size is large.

2. Crossover Types

- **Scattered**

Scatter derives its bases from earlier strategies for setting up constraints and decision regulations. The aim of this type of crossover enables a solution procedure based on the elements which are combined to provide better individuals than one based only on the parent elements.

3. Mutation

- **Uniform**

A mutation operator is used to replace the value of the chosen property with a uniform random value selected between the specified upper and lower bounds. This mutation operator is suitable for float and integer properties (genes).

- **Gaussian**

A mutation operator is used for adding a unit Gaussian distributed random value to the chosen gene. Clipping is required for the new gene if it is not between the specified value lower or upper bounds for that gene. This mutation is suitable for float and integer properties (genes).

4. Elitism

In the generation, some individuals may have better fitness value than the other individuals. Therefore, in order to avoid destruction of these individuals due to the crossover and mutation operator, they should be passed to the new generation without any changes. Elitisit selection is used for choosing the best individuals and passing them to the new generation. However, the number of elitist selection should not be too high, otherwise the generations cycles aroud the elitist individuals.